ACS OMEGA

Open Access

http://pubs.acs.org/journal/acsodf

Article

Novel Lawsone–Quinoxaline Hybrids as New Dual Binding Site Acetylcholinesterase Inhibitors

Paptawan Suwanhom, Teerapat Nualnoi, Pasarat Khongkow, Varomyalin Tipmanee,* and Luelak Lomlim*

Cite This: *ACS Omega* 2023, 8, 32498–32511

Read Online

ACCESS | Metrics & More | Article Recommendations | Supporting Information

ABSTRACT: A new family of lawsone–quinoxaline hybrids was designed, synthesized, and evaluated as dual binding site cholinesterase inhibitors (ChEIs). *In vitro* tests revealed that compound **6d** was the most potent AChEI (IC_{50} = 20 nM) and BChEI (IC_{50} = 220 nM). The compound **6d** did not show cytotoxicity against the SH-SY5Y neuronal cells (GI_{50} > 100 μM). *In silico* and enzyme kinetic experiments demonstrated that compound **6d** bound to both the catalytic anionic site and the peripheral anionic site of *Hu*AChE. The lawsone–quinoxaline hybrids exhibited potential for further development of potent acetylcholinesterase inhibitors for the treatment of Alzheimer's disease.

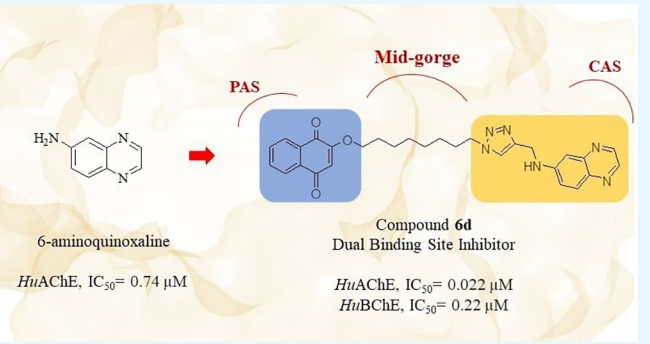

1. INTRODUCTION

Alzheimer's disease (AD) is a neurodegenerative disorder that impairs cognitive function as well as other behavioral abilities. As the major form of dementia, it currently affects 55 million senior people globally, with the number expected to climb to 78 million by 2030.[1] As the world's population ages, effective anti-Alzheimer agents are still required. Among the pathological hallmarks of AD are decreased levels of the cholinergic neurotransmitter acetylcholine (ACh), hyperphosphorylation of the tau protein, beta-amyloid protein deposition, biometal imbalances, oxidative stress, and neuroinflammation.[2,3] The most widely recognized hypothesis for the discovery of anti-AD medications is the cholinergic hypothesis.

Acetylcholinesterase (AChE: EC 3.1.1.7) is a serine hydrolase that is responsible for ACh activity termination. The catalysis of ACh occurs at the bottom of the 20 Å deep active site gorge by the action of Ser203, which forms a catalytic triad (CT) with His447 and Glu334. Near the CT, there are the catalytic anionic site (CAS) and acyl pocket. The peripheral anionic site (PAS) is located at the entrance of the active site gorge and is made up of several aromatic amino acids.[4] Butyrylcholinesterase (BChE, EC 3.1.1.8) is another ACh-degrading enzyme widely distributed in the body.[5] In a healthy brain, AChE plays the principal role in ACh hydrolysis. However, in the individuals with progressing AD, the level of BChE significantly increased.[6] AChE and BChE inhibitors (AChEI and BChEI), which can raise brain ACh levels, have thus been the focus of the treatment for AD.[7] Due to their capacity to reinforce the cholinergic neurotransmitter system, acetylcholinesterase inhibitors (AChEIs) have been approved by the Food and Drug Administration (FDA) for the treatment of AD since 1993, in the case of tacrine. However, these medications have so far only been able to temporarily reduce AD symptoms; therefore, there is still a need for new effective anti-AD agents.[8]

X-ray crystallographic studies revealed that some approved AChEIs, such as tacrine and galanthamine, bound to the CAS region and prevented ACh from reaching the CT, thus reducing the rate of ACh hydrolysis.[9] Donepezil can interact with both the CAS and PAS sites and show excellent potency in AChE inhibition and increased AChE selectivity.[10] The dual binding site inhibitors have been recognized as an approach to find the promising anti-AD candidates in the search for more effective anti-Alzheimer's agents. One strategy for developing a potent dual-binding site inhibitor is to design hybrid molecules made of CAS and PAS ligands linked together with an appropriate linker.[11−20] Our group reported new quinoxaline derivatives as potent acetylcholinesterase inhibitors. *In silico* studies suggested that the quinoxaline derivatives interacted with the amino acids in the PAS.[21] To discover AChEIs with greater efficacy, we further developed lawsone–quinoxaline hybrids as dual binding site inhibitors in this study.

Received: April 19, 2023
Accepted: August 15, 2023
Published: August 29, 2023

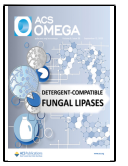

Naphthoquinones (NQs) are extensively distributed in nature and showed significant biological activities. Recent studies have also shed light on the neuroprotective effects, acetylcholinesterase inhibition, and Aβ aggregation inhibition performed by 1,4-NQ-derived compounds.[22−25] Lawsone (2-hydroxy-1,4-napthoquinone) is the main natural dye from the leaves of Henna plants.[26] AChEI activity of some synthetic lawsone derivatives and lawsone-like derivatives was reported.[27−29] According to the *in silico* simulations, the 1,4-NQ system interacted with amino acid residues along the AChE active site gorge.[27,28] The para-quinone moiety primarily interacted with the amino acid residues at the CAS site, while the aromatic ring interacted with the amino acid residues in the PAS.[22,23] Therefore, lawsone was proposed to be a CAS ligand for the design of the hybrid molecule that act as dual binding site AChE inhibitors.

The 6-aminoquinoxaline moiety could serve as a PAS ligand,[21] whereas the lawsone molecule could be a promising candidate for CAS binding.[22,23] This led to the new idea of connecting both moieties via the linker to generate the synthesized compound that could act as the dual site-bound ligand to increase inhibitory efficacy. In this study, we designed and synthesized new hybrids of lawsone and quinoxaline as dual-binding site acetylcholinesterase inhibitors. A lawsone molecule (as the CAS ligand) and 6-aminoquinoxaline moiety (as the PAS ligand) were linked together via a 1,2,3-triazole linker. The optimal linker length to permit interactions with both CAS and PAS sites was determined by varying the length of the methylene chain.

The 1,2,3-triazole heterocycle has been widely used in drug design, including new dual binding site AChE inhibitors, due to its facile synthesis, low toxicity, good pharmacokinetic profile, and resistance to acidic or basic conditions. The nitrogen atoms in the 1,2,3-triazole ring also contributed to enzyme−inhibitor interactions.[30] The synthesized compounds were evaluated for AChE and BChE inhibition. The inhibition mode of the active compound was determined by the enzyme kinetic study. In-depth binding interactions between the inhibitor and the enzymes were explored by *in silico* studies. The cytotoxicity of the synthesized compounds was evaluated in neuronal cells. The rationale for the design of the lawsone−quinoxaline hybrids is illustrated in Figure 1.

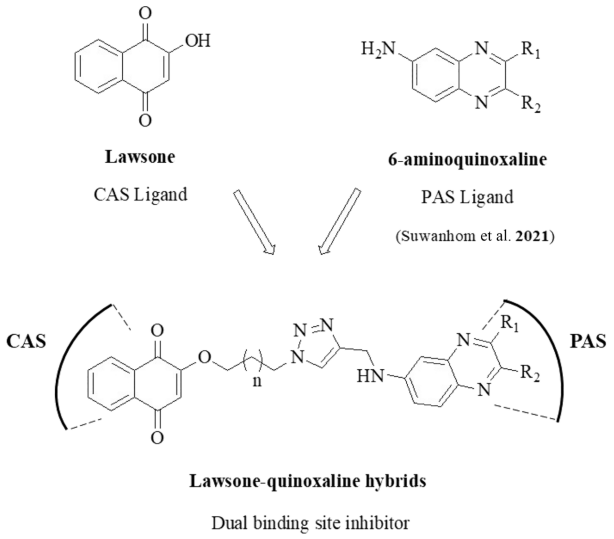

Figure 1. Conceptual design for the lawsone−quinoxaline hybrids.

2. RESULTS AND DISCUSSION

2.1. Chemistry. The synthesis of lawsone−quinoxaline hybrids (**6a-8d**) was conducted according to the steps shown in Scheme 1. The starting materials, 6-aminoquinoxaline derivatives (**1a-1c**), were prepared as described in the literature.[21] Initially, compounds **1a-1c** were treated with propargyl bromide under basic conditions to afford *N*-(prop-2-ynyl)naphthalen-2-amine derivatives (**2a-2c**) under the conditions previously reported.[31] Lawsone (**3**) was reacted with a solution of the corresponding dichloroalkane in basic conditions, in the presence of KI and a phase-transfer catalyst to yield **4a-4d**.[32] Then, **4a-4d** were further reacted with NaN_3 to yield azidoalkyl derivatives of lawsone (**5a-5d**) as previously reported.[33] Finally, **5a-5d** and **2a-2c** underwent cyclization via copper-catalyzed azide−alkyne cycloaddition (Cu-AAC) reactions to yield the desired lawsone−quinoxaline hybrids (**6a-8d**) in moderate to good yield.[34]

2.2. Biological Activities. *2.2.1. In Vitro Enzyme Inhibition Assays.* The lawsone−quinoxaline hybrids (**6a-8d**) were evaluated *in vitro* for their anti-cholinesterase activity against AChE and BChE in comparison to the reference drugs tacrine and donepezil (Table 1). For cholinesterase, Ellman's method[35,36] was used to assess the inhibition potential of these compounds against human AChE (*Hu*AChE) and BChE from equine serum (*Eq*BChE).

Table 1 summarizes the lawsone−quinoxaline hybrid anti-cholinesterase activities. To better understand the structure−activity relationships (SARs), the synthesized compounds were divided into three groups: compounds **6a-6d**, **7a-7d**, and **8a-8d**. In the first group, compound **6d**, possessing a methylene linker (n = 6) and an unsubstituted quinoxaline moiety, displayed excellent AChE inhibitory activity with an IC_{50} value of 0.022 ± 0.004 μM. This was much more active than tacrine. However, it was still less potent than donepezil (IC_{50} = 0.006 ± 0.0006 μM). AChEI activity was reduced when the length of the methylene linker was deleted (as in compounds **6a**, **6b**, and **6c**). In the second group, compounds **7a** (n = 1) and **7b** (n = 2) were found to be moderately potent AChE inhibitors (IC_{50} = 3.6 ± 1.2 μM and IC_{50} = 7.1 ± 1.2 μM, respectively), while compounds **7c** and **7d** showed no inhibitory activity (IC_{50} > 100 μM). Considering the inhibitory activity of compounds **8a-8d** in the third group, compound **8d** showed the most potent activity with an IC_{50} value of 3.5 ± 0.3 μM.

Meanwhile, compounds **8a**, **8b**, and **8c** exhibited decreased activity because of a shorter methylene linker. For anti-BChE activity, the presence of hydrogen atoms at R_1 and R_2 positions on the quinoxaline ring, linker n = 6 (**6d**), led to relatively good activity (IC_{50} = 0.22 ± 0.02 μM). This compound exhibited higher potency than donepezil (IC_{50} = 1.8 ± 0.5 μM) but lower potency than tacrine (IC_{50} = 0.017 ± 0.0006 μM). The substitution of quinoxaline with a phenyl at the R_1 position (as in compounds **7a-7d**) or a dimethyl group on the R_1 and R_2 positions (as in compounds **8a-8d**) led to decreased BChE activity. When the selectivity index (SI) was compared with those of the AChE-selective drug, donepezil (SI = 300), and the non-selective cholinesterase inhibitors (tacrine; SI = 0.1), the lawsone−quinoxaline hybrids tended to be non-selective cholinesterase inhibitors. Owing to the remarkable inhibitory activity on both AChE and BChE, compound **6d** needs further intensive investigation.

According to Table 1, we found that the inclusion of a phenyl group in the quinoxaline ring and a longer linker carbon

https://doi.org/10.1021/acsomega.3c02683
ACS Omega 2023, 8, 32498−32511

Scheme 1. Synthesis of the Lawsone−Quinoxaline Hybrids (6a-8d)[a]

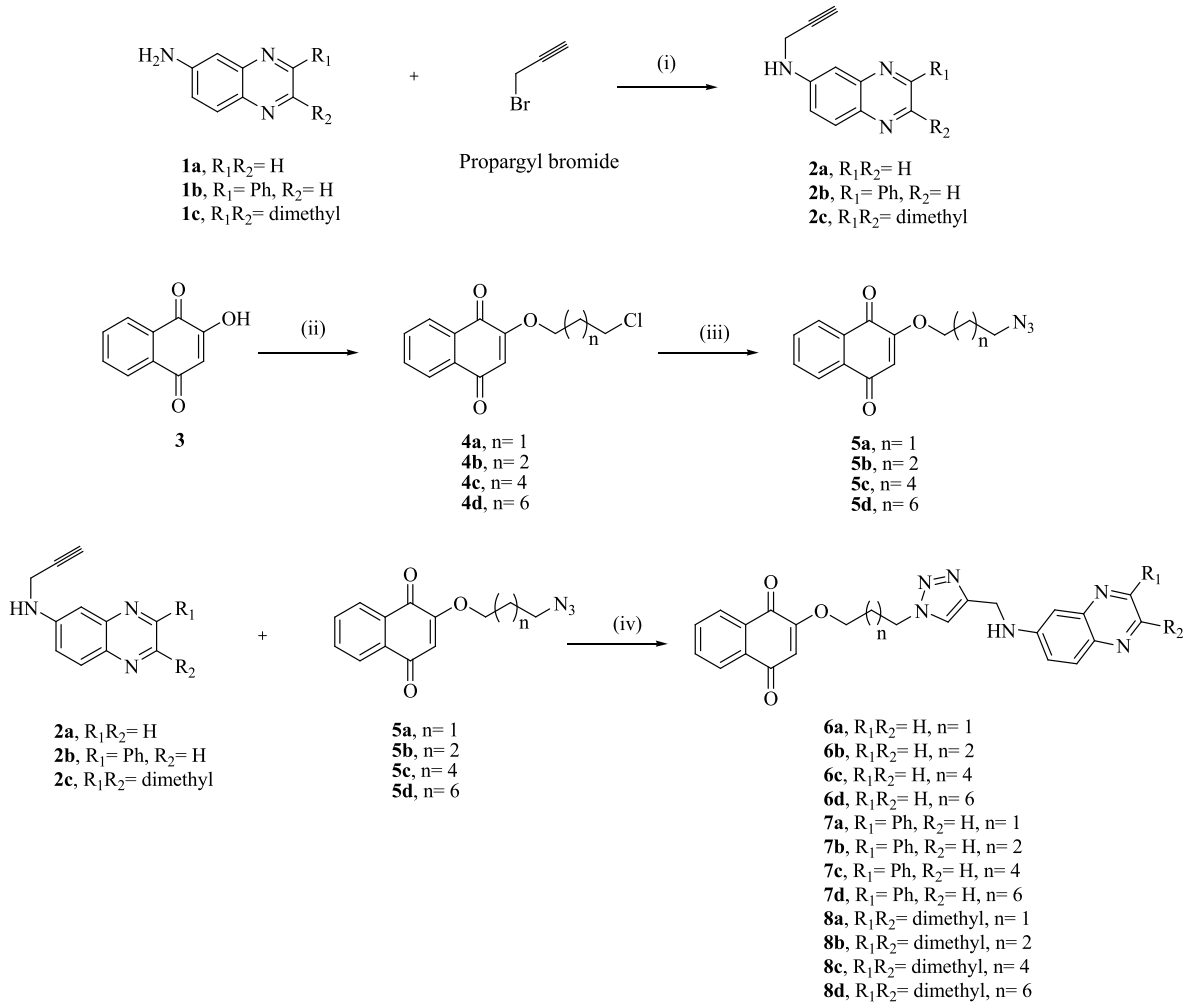

[a]Reaction conditions: (i) KI, K_2CO_3, DMF, 80 °C; (ii) dichloroalkane, K_2CO_3, ACN, 80 °C; (iii) NaN_3, EtOH, 120 °C; (iv) $CuSO_4{\cdot}5H_2O$, Cu-powder, EtOH, rt.

chain could reduce the AChE and BChE activities, compared to the non-existence of the phenyl group (**6d**). The reason can be speculated from the intramolecular $\pi-\pi$ stacking of the molecule. The carbon linker in compounds **6d** and **7d** is identical; however, only **7d** could preferably form intramolecular $\pi-\pi$ stacking as both aromatic moieties and a long linker. The phenyl group is present in **7b** as well as **7d**, but the shorter linker does not allow for intramolecular stacking. This could explain why the molecules were less able to stretch to fit the AChE gorge site when the phenyl group was located at the quinoxaline ring. The figure of this speculated statement is provided in the Supporting Information.

2.2.2. Determination of Kinetic Parameters for Compound ***6d****.* The kinetic behavior of the most active compound, **6d**, was investigated using Ellman's method. There were reciprocal Lineweaver−Burk plots between 1/velocity at the *Y* axis against the increasing concentration of 1/substrate (ATChI: 0.5, 1.5, 5.0, and 10 μM) at the *X* axis in the presence of different inhibitor concentrations (0, 4, 7.5, and 15 μM). After being calculated by the Prism software, compound **6d** exhibited a mixed-type inhibition pattern (Figure 2). Also, alpha data shown at 4.18 was greater than one; this meant that the inhibitor was preferentially bound to the free enzyme. Both increasing slopes (decreased V_{max}) and intercepts (increased K_m) suggested that **6d** might be able to bind the PAS as well as the CAS of AChE.

2.2.3. In Vitro Cytotoxicity Evaluation. SH-SY5Y is a standard cell line used for establishing the neurotoxic effect of a potential drug and a well-founded *in vitro* model of neurodegenerative disorders.[38−40] SRB assays were performed to evaluate the cytotoxicity of our compounds at various concentrations, varying from 3.125 to 100 μM, on SH-SY5Y neuron cells. The GI_{50} values were determined as the half-maximal inhibitory concentration of cell growth. As shown in Table 2, the results demonstrated that most of these compounds at all concentrations up to 100 μM, except **8a** and **8b**, did not show significant toxicity to the SH-SY5Y (GI_{50} > 90 μM), while donepezil, as a reference drug, showed a GI_{50} value of 92.67 ± 8.49 μM. Compound **6d** exhibited AChE inhibitory activity with an IC_{50} value of 22 nM (Table 1) but became cytotoxic to half of the SH-SY5Y cells at more than a 4500 times higher concentration; therefore, this compound was considered to be non-toxic to the neuronal cells.

2.3. *In Silico* Analysis of ChE Inhibition Characteristics of Compound 6d. Because of the remarkable AChE and BChE inhibition activity of compound **6d**, an *in silico* study was performed to understand the inhibition mechanism within the

https://doi.org/10.1021/acsomega.3c02683
ACS Omega 2023, 8, 32498−32511

Table 1. Inhibitory Activity against AChE and BChE by Compounds 6a-8d

Cpd.	*n*	R_1	R_2	AChE IC_{50} ±SD (μM)[a]	BChE IC_{50} ± SD (μM)[b]	SI[c]
6a	1	H	H	16.2 ± 0.4	15.4 ± 1.2	0.95
6b	2	H	H	31.1 ± 0.6	35.5 ± 0.9	1.14
6c	4	H	H	0.58 ± 0.05	1.4 ± 0.3	2.41
6d	6	H	H	0.022 ± 0.004	0.22 ± 0.02	10
7a	1	Ph	H	3.6 ± 1.2	>100	>27.78
7b	2	Ph	H	7.1 ± 1.2	>100	>14.08
7c	4	Ph	H	>100	>100	
7d	6	Ph	H	>100	4.4 ± 0.4	<0.044
8a	1	CH_3	CH_3	5.4 ± 0.4	>100	>18.52
8b	2	CH_3	CH_3	15.5 ± 0.6	>100	>6.45
8c	4	CH_3	CH_3	9.0 ± 0.9	3.8 ± 0.3	0.42
8d	6	CH_3	CH_3	3.5 ± 0.3	1.7 ± 0.3	0.49
tacrine				0.17 ± 0.01 (0.11 ± 0.01)[21]	0.017 ± 0.0006 (0.006 ± 0.001)[21]	0.1
donepezil				0.006 ± 0.0006 (0.004 ± 0.0001)[32]	1.8 ± 0.5 (1.42)[37]	300

[a]Human recombinant AChE. [b]BChE from equine serum. [c]Selectivity index = BChE IC_{50}/AChE IC_{50}.

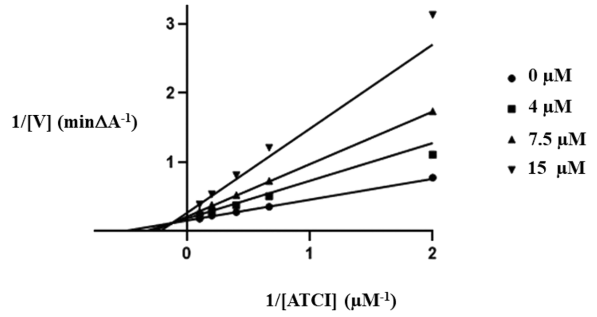

Figure 2. Lineweaver–Burk plot for the inhibition of AChE by compound **6d**.

Table 2. GI_{50} (μM) Values of Selected Lawsone–Quinoxaline Hybrids (6a-8d) in the SH-SY5Y Cell Line

Cpd.	GI_{50} ± SD (μM)
6a	93.98 ± 8.89
6b	93.19 ± 9.54
6c	>100
6d	>100
7a	>100
7b	>100
7c	>100
7d	>100
8a	31.18 ± 14.30
8b	42.60 ± 10.00
8c	>100
8d	>100
donepezil	92.67 ± 8.49

active site of the target enzymes (*Hu*AChE: PDB ID: 7D9O and *Hu*BChE: PDB ID: 4BDS).

2.3.1. Molecular Docking Studies of the AChE and BChE Enzyme. Molecular docking experiments were performed on the AChE and BChE enzyme crystal structures to illustrate how the active compound **6d** and donepezil interacted with the active site gorge. The **6d** and donepezil were considered. From the molecular docking results, compound **6d** has shown comparable interactions with AChE and BChE with donepezil. The docking scores of **6d** against AChE and BChE are given in Table 3.

Table 3. Docking Scores (kcal/mol) of 6d and Donepezil (*Hu*AChE and *Hu*BChE)

Cpd.	docking score to AChE (kcal/mol)[a]	docking score to BChE (kcal/mol)[b]
6d	−11.56	−10.29
donepezil	−11.46	−10.64

[a]Human recombinant AChE (PDB ID: 7D9O). [b]Human BChE (PDB ID: 4BDS).

The **6d** interacted with important amino acid residues in the AChE enzyme pocket site with a binding free energy of −11.56 kcal/mol. The quinoxaline ring formed a $\pi-\pi$ stack with the Trp80 (a key residue in the CAS of AChE), and the 6-NH group on the quinoxaline ring displayed a hydrogen bond with Gly114, as shown in Figure 3a. The naphthoquinone ring of the lawsone moiety also formed a $\pi-\pi$ interaction with Trp280 (a key residue in the PAS of AChE) and Tyr118. Furthermore, the triazole group formed a $\pi-\pi$ interaction with Trp80. A methylene chain is located in the *Hu*AChE mid-gorge between CAS and PAS. This chain formed an π-alkyl interaction with Tyr331 and Tyr335. Therefore, **6d** could bind both *Hu*AChE sites, consistent with the kinetic result.

Similarly, donepezil also showed interactions with the active site of AChE with a docking score of −11.46 kcal/mol. The benzyl piperidine core of donepezil is surrounded by CAS pocket residues, while the indanone ring is oriented toward the PAS pocket (Figure 3b). The benzyl group formed a $\pi-\pi$ interaction with Trp80. The nitrogen atom of the piperidine ring also formed a cation-π interaction with Tyr331. The $\pi-\pi$ bond was observed between the piperidine ring and Tyr332. The carbonyl group of the indanone ring showed a hydrogen bond with Phe289. In addition, the indanone ring interacted with Trp280 and Tyr335. Also, the methoxy group formed a hydrogen bond with Tyr335.

For BChE, compound **6d** (−10.29 kcal/mol) exhibited similar interaction modes as the reference compound (−10.64 kcal/mol). The $\pi-\pi$ bond has been formed by the quinoxaline ring of the ligand with the amino acid residue Tyr332 in Figure 3c. The 6-NH group displayed a hydrogen bond with Thr120. The triazole ring established a $\pi-\pi$ interaction with the Trp82. The interaction of the lawsone ring is important for binding to CAS. The lawsone moiety constitutes a hydrogen bond formation between the carbonyl of the lawsone and the amino acid of Thr128, and the lawsone ring also formed a $\pi-\pi$ interaction with Trp82. Furthermore, the π-alkyl bond has been formed between the methylene chain and Trp430.

The docking pose of donepezil with the BChE enzyme revealed that the benzyl ring displayed $\pi-\pi$ interaction with Trp82. The $\pi-\pi$ bond was observed between the indanone ring with the Tyr332, and the carbonyl group of the indanone ring exhibited a hydrogen bond with Trp82, as shown in Figure 3d.

In this study, we used BChE isolated from horse serum for *in vitro* assays and human BChE for *in silico* research. We compared CAS and PAS sites across species using sequence alignment to see if they were similar. According to the

https://doi.org/10.1021/acsomega.3c02683
ACS Omega 2023, 8, 32498−32511

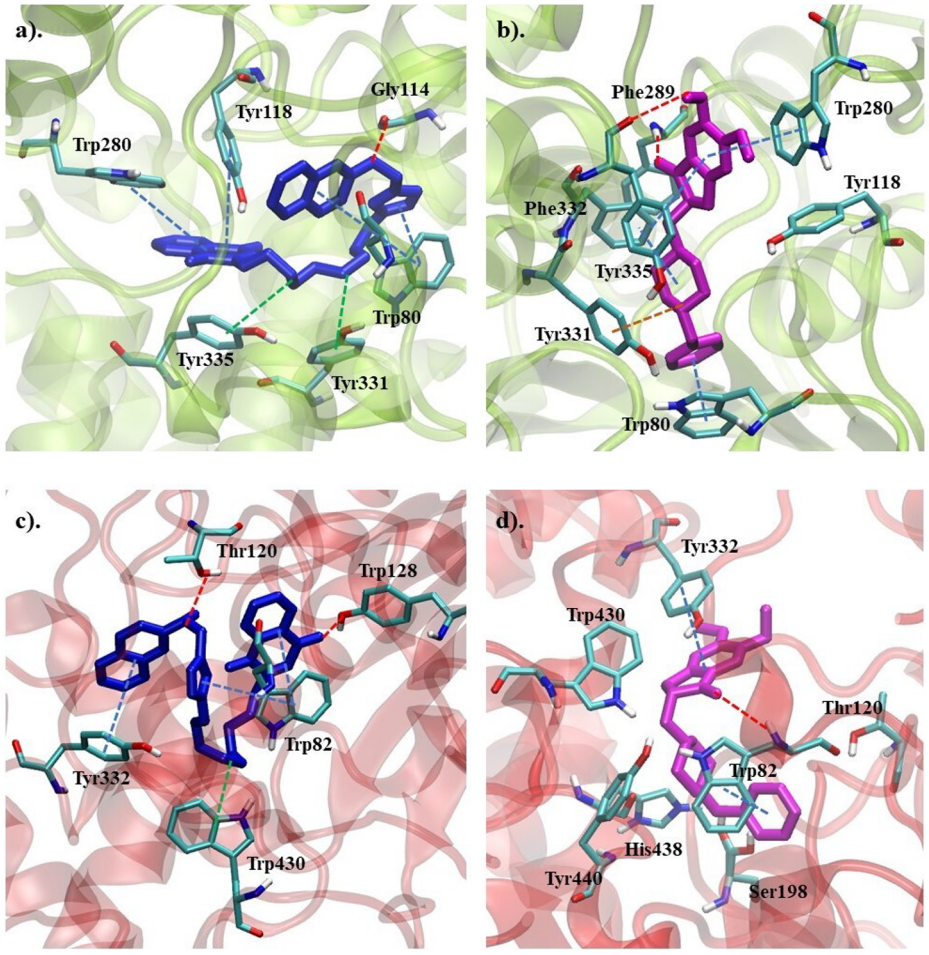

Figure 3. Molecular docking of **6d** and donepezil with AChE and BChE. (a) Predicted binding modes of **6d** and AChE (PDB ID: 7D9O). (b) Predicted binding modes of donepezil and AChE (PDB ID: 7D9O). (c) Predicted binding modes of **6d** and BChE (PDB ID: 4BDS). (d) Predicted binding modes of donepezil and BChE (PDB ID: 4BDS). The red color represents hydrogen bonding interactions, the blue color represents $\pi-\pi$ interactions, the green color represents π-alkyl interactions, and the brown color represents cation-π interactions.

supplementary materials, we found that the two enzymes are more than 90% similar. These may provide justification for, or at least a hint toward, comparing horse BChE results to human BChE *in silico* results.

2.3.2. Conceptual Summary. The binding pattern of **6d** was analyzed in the active site gorge to understand dual binding site properties: PAS and CAS. When the docking pose of compound **6d** was examined, it was detected that it was bound to the enzymes in a location similar to that of donepezil. The hydrogen bonds and $\pi-\pi$ interactions were assumed to be key factors for its binding. We expected that the lawsone ring (CAS ligand) and quinoxaline ring (PAS ligand) were linked together via a 1,2,3-triazole linker. A quinoxaline ring is mostly surrounded by residues of the CAS pocket, while a lawsone ring is oriented toward the PAS pocket for the *Hu*AChE enzyme. In contrast, lawsone is oriented toward the CAS and the quinoxaline ring is located in the PAS site for *Hu*BChE. Meanwhile, the 1,2,3-triazole group interacted in the CAS site via $\pi-\pi$ interaction with Trp (Trp80 for AChE and Trp82 for BChE).

2.3.3. Molecular Dynamics Simulation. Molecular dynamics (MD) simulations were investigated for the stability of the docking complexes of **6d** and donepezil with *Hu*AChE. The root mean square distance (RMSD) values were monitored to measure the stability of the ligand and protein that they possess. In this study, we found that RMSD values of **6d**-*Hu*AChE and donepezil-*Hu*AChE complexes displayed system stability after the system was run for 200 ns (Figure 4). The relative binding energy of **6d** and donepezil was calculated using molecular mechanics Poisson−Boltzmann surface area (MM-PBSA). Table 4 shows values of −63.73 ± 0.16 and −40.78 ± 0.15 kcal/mol, respectively.

Additionally, **6d** and donepezil specifically interacted with *Hu*AChE through Trp. An analysis revealed that both compounds formed $\pi-\pi$ interactions through Trp80 and Trp280 (Figure 5b,d). These amino acids are the key amino acid residues in the active site of the enzyme (Trp80: CAS and Trp280: PAS). The result displayed that the RMSD of all compounds presented relatively stable fluctuations within the 150 ns MD simulation, indicating that the simulated system has basically reached equilibrium (Figure 5a,c).

The difference in the relative binding energy of **6d** and donepezil was due to the $\pi-\pi$ interactions. Even though both can perform the $\pi-\pi$ stacking, **6d** could form both sandwich-like stacking with Trp280 and Trp80 (Figure 5b), while donepezil could form only sandwich-like stacking with Trp280. The other $\pi-\pi$ stacking of donepezil to Trp80 was t-shaped, a less preferable interaction (Figure 5d). Furthermore, the sandwich-liked interaction of **6d** occurred at a closer distance

https://doi.org/10.1021/acsomega.3c02683
ACS Omega 2023, 8, 32498−32511

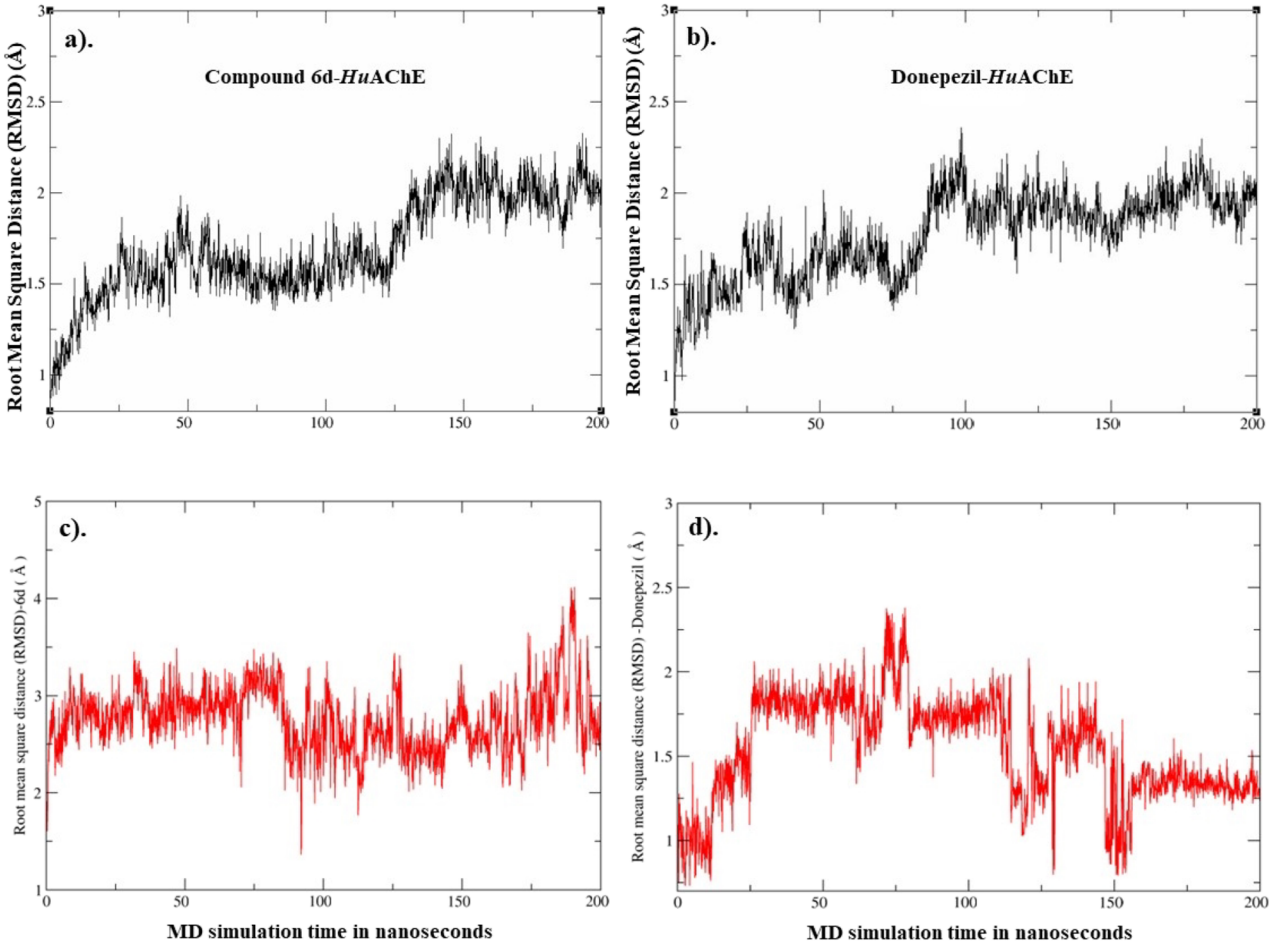

Figure 4. RMSD plot of MD simulations versus simulation time. The MD trajectory consisted of 2000 equidistant snapshots taken from a simulation of 200 ns. Based on the protein backbone atoms (N, C, and Cα), the RMSD was plotted using the crystal structure PDB ID: 7D9O. The RMSD of the ligand (**6d** or donepezil) was based on all atoms except hydrogen, from the docked pose. (a) Compound **6d**-*Hu*AChE, (b) donepezil-*Hu*AChE, (c) compound **6d**, and (d) donepezil.

Table 4. MM-GBSA Relative Binding Energy (kcal/mol) of Compound 6d and Donepezil (*Hu*AChE)

Cpd.	MM-GBSA relative binding energy to AChE (kcal/mol)[a]
6d	−63.73 ± 0.16
donepezil	−40.78 ± 0.15

[a]Human recombinant AChE (PDB ID: 7D9O).

compared to donepezil (Figure 5a,c), suggesting a stronger interaction leading to the lower binding energy of **6d**.

3. CONCLUSIONS

In summary, a novel series of lawsone−quinoxaline derivatives were successfully designed and synthesized by click chemistry as efficient for the treatment of AD. All the target compounds were synthesized and screened as ChE inhibitors. Most of the synthesized compounds displayed moderate to excellent AChEI and BChEI activity. Our results showed that compound **6d** binds to both CAS and PAS in the active sites of AChE and BChE, which implies that these compounds could act as dual binding site inhibitors. Finally, the results suggest that these new compounds could be considered as a new lead for further development of potent ChEIs for treatment of AD.

4. EXPERIMENTAL SECTION

4.1. Chemistry. Lawsone (**3**), dimethylformamide (DMF), benzyltriethylammonium chloride (TEBAC), and all other starting materials, solvents, and reagents were purchased from commercial sources. ^{1}H-NMR and ^{13}C-NMR spectra were recorded in $CDCl_3$ or DMSO-d_6 on a Varian Unity Inova 500 MHz instrument. The chemical shifts (δ) and coupling constants (J) were represented in parts per million (ppm) and hertz (Hz), respectively. Mass spectral analyses (ESI-MS) were carried out by a Thermo Finnigan MAT 95XL and Agilent Technology G6545A. Column chromatography was performed on silica gel 60 Å, 60−200 μm from SiliCycle Inc. (Quebec City, Canada). Thin-layer chromatography (TLC) was performed on 20 cm × 20 cm (0.2 mm) precoated silica gel plates (Aluminum Oxide 60 Neutral F_{254}).

*4.1.1. General Procedure for the Synthesis of N-(Prop-2-ynyl)naphthalen-2-amine Derivatives (**2a-2c**).* Derivatives of 6-aminoquinoxaline (**1a-1c**, 2.5 mmol) were exactly prepared according to the literature,[15] K_2CO_3 (3.5 mmol) and propargyl bromide (3.5 mmol) were added to a round-bottom flask, and 10 mL of dry DMF was added as a solvent and refluxed at 80 °C overnight. After the reaction was monitored by TLC, the reaction was terminated, quenched with water, and extracted with ethyl acetate (EtOAc, 50 mL, three times). The combined organic layer was washed with distilled water (10 mL, two

https://doi.org/10.1021/acsomega.3c02683
ACS Omega 2023, 8, 32498−32511

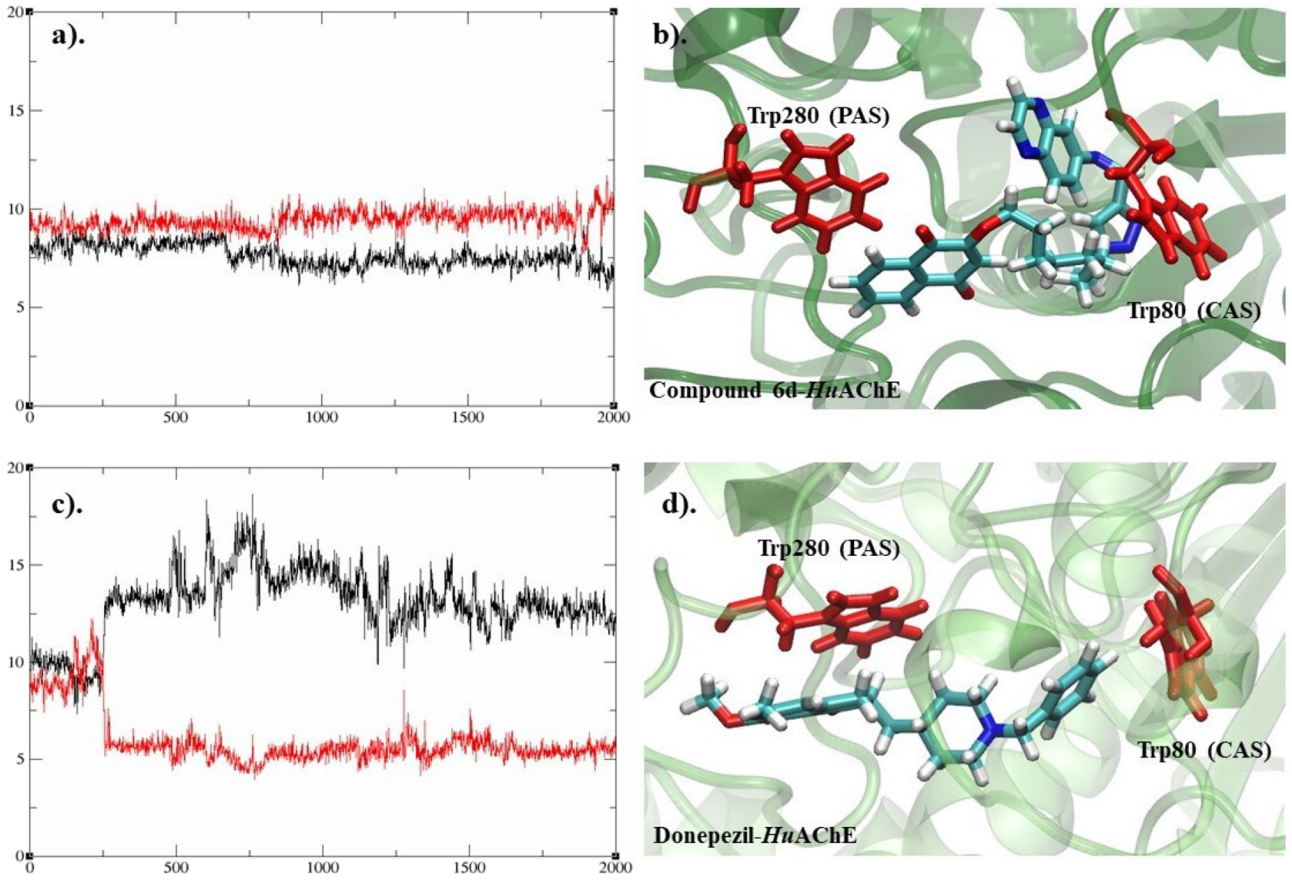

Figure 5. RMSD graph and distance plot. For 200 ns, the plot contained 2000 snapshots from the simulation. After 150 ns, the distance between compound **6d** and donepezil with Trp80 and Trp280 became constant, implying that the compounds remained with Trp80 and Trp280; (a) distance plot between compound **6d** with Trp80 (CAS) and Trp280 (PAS). (b) Interaction between compound **6d** and *Hu*AChE. (c) Distance plot between donepezil with Trp80 (CAS) and Trp280 (PAS). (d) Interaction between donepezil and *Hu*AChE (black line for Trp80, red line for Trp280).

times) and brine (10 mL). Trace of water remaining in the organic layer was removed by addition of Na_2SO_4. The product was purified by column chromatography over silica gel to furnish the pure product using EtOAc:hexane (40:60) as the mobile phase and recrystallized from EtOAc. The products were characterized by the corresponding spectroscopic data (^{1}H-NMR, ^{13}C-NMR, and ESI-MS of each compound are in the Supporting Information).

*4.1.1.1. N-(Prop-2-ynyl)quinoxaline-6-amine (**2a**).* Compound **2a** was obtained from compound **1a** and propargyl bromide as described in the general procedure. Yellow solid; yield 68%; IR (KBr): 3433.7, 3298.1, 3216.7, 1622.9, 1533.9, 1441.8, 1237.9, 953.9, 857.5 cm^{-1}. ^{1}H-NMR (500 MHz, DMSO-d_6): δ 8.68 (1H, d, J = 2.0 Hz, H2), 8.53 (1H, d, J = 2.0 Hz, H3), 7.80 (1H, d, J = 9.10 Hz, H5), 7.32 (1H, dd, J = 2.60, 9.10 Hz, H8), 7.00 (1H, t, J = 5.80 Hz, NH), 6.93 (1H, d, J = 2.54 Hz, H6), 4.06 (2H, dd, J = 2.40, 5.80 Hz, CH_2), 3.16 (1H, t, J = 2.40 Hz, CH). ^{13}C-NMR (125 MHz, DMSO-d_6): δ 149.37, 145.54, 145.29, 140.78, 137.49, 129.90, 122.94, 103.55, 81.62, 74.00, 32.43. ESI-MS: calcd. for $C_{11}H_9N_3$ [M + H]$^+$: 184.0869, found: 184.0869.

*4.1.1.2. 3-Phenyl-N-(prop-2-ynyl)quinoxaline-6-amine (**2b**).* Compound **2b** was obtained from compound **1b** and propargyl bromide as described in the general procedure. Yellow solid; yield 62%; IR (KBr): 3450.2, 2950.3, 2935.9, 1738.0, 1623.9, 1432.2, 1216.9, 916.1, 690.0 cm^{-1}. ^{1}H-NMR (500 MHz, DMSO-d_6): δ 9.43 (1H, s, H3), 8.28 (2H, d, J = 7.3 Hz, H1′, H5′), 8.02 (1H, d, J = 9.30 Hz, H5), 7.70 (1H, dd, J = 2.80, 9.30 Hz, H8), 7.55 (4H, m, H2′, H3′, H4′, NH), 7.35 (1H, d, J = 2.80 Hz, H6), 4.41 (2H, d, J = 2.20 Hz, CH_2), 3.25 (1H, t, J = 2.20 Hz, CH). ^{13}C-NMR (125 MHz, DMSO-d_6): δ 148.38, 148.03, 143.98, 143.03, 136.99, 136.49, 130.08, 130.04, 129.51, 127.26, 121.96, 109.04, 80.01, 75.84, 40.62. ESI-MS: calcd. for $C_{17}H_{13}N_3$ [M + H]$^+$: 260.1182, found: 260.1185.

*4.1.1.3. 2,3-Dimethyl-N-(prop-2-ynyl)quinoxaline-6-amine (**2c**).* Compound **2c** was obtained from compound **1c** and propargyl bromide as described in the general procedure. Yellow solid; yield 69%; IR (KBr): 3263.2, 3191.4, 3051.1, 1622.4, 1510.8, 1441.7, 1246.9, 994.2, 709.4 cm^{-1}. ^{1}H-NMR (500 MHz, DMSO-d_6): δ 7.82 (1H, d, J = 9.20 Hz, H5), 7.51 (1H, dd, J = 2.80, 9.20 Hz, H8), 7.23 (1H, d, J = 2.80 Hz, H6), 4.33 (3H, m, NH, CH_2), 3.21 (1H, t, J = 2.30 Hz, CH), 2.61 (6H, d, J = 8.20 Hz, 2 × CH_3). ^{13}C-NMR (125 MHz, DMSO-d_6): δ 154.09, 150.43, 147.65, 142.17, 135.44, 128.73, 120.06, 109.28, 80.13, 75.71, 40.58, 23.16, 22.80. ESI-MS: calcd. for $C_{13}H_{13}N_3$ [M + H]$^+$: 212.1182, found: 212.1182.

*4.1.2. General Procedure for the Synthesis of Chloroalkyl Derivatives of Lawsone (**4a-4d**).* To a solution of lawsone (**3**, 10 mmol) in acetonitrile (CH_3CN, 20 mL), KI (1.6 mmol), K_2CO_3 (10 mmol), TEBAC (10 mmol) in CH_3CN (20 mL), and a solution of corresponding dichloroalkane (50 mmol) dissolved in 10 mL of CH_3CN were added, and the mixture was heated at reflux 80 °C for 24 h. After the reaction was

https://doi.org/10.1021/acsomega.3c02683
ACS Omega 2023, 8, 32498−32511

monitored by TLC, the reaction mixture was then cooled to room temperature. The solid was filtered off, and the filtrate was collected and evaporated. The obtained crude product was purified by column chromatography on silica gel to furnish the pure product using EtOAc:hexane (20:80) as the mobile phase and recrystallized from CH_2Cl_2. The products were characterized by the corresponding spectroscopic data (^{1}H-NMR, ^{13}C-NMR, and ESI-MS of each compound are provided in the Supporting Information).

*4.1.2.1. 2-(3-Chloropropoxy)naphthalene-1,4-dione (**4a**).* Compound **4a** was obtained from lawsone (**3**) and 1,3-dichloropropane as described in the general procedure. Yellow solid; yield 81%; IR (KBr): 3056.2, 2963.4, 1686.3, 1608.5, 1332.3, 1018.3, 879.0, 723.1 cm^{-1}. ^{1}H-NMR (500 MHz, DMSO-d_6): δ 8.11 (2H, m, H5, H8), 7.74 (2H, m, H6, H7), 6.20 (1H, s, H3), 4.17 (2H, t, J = 5.87 Hz, H1′), 3.78 (2H, t, J = 6.11 Hz, H2′), 2.36 (2H, m, H3′). ^{13}C-NMR (125 MHz, DMSO-d_6): δ 184.90), 179.93, 159.51, 134.33, 133.37, 131.98, 131.12, 126.69, 126.20, 110.53, 65.69, 40.93, 31.23. ESI-MS: calcd. for $C_{13}H_{11}ClO_3$ [M + H]$^+$: 251.0469, found: 251.0469.

*4.1.2.2. 2-(4-Chlorobutoxy)naphthalene-1,4-dione (**4b**).* Compound **4b** was obtained from lawsone (**3**) and 1,4-dichlorobutane as described in the general procedure. Yellow solid; yield 79%; IR (KBr): 3055.5, 2939.0, 1685.1, 1655.1, 1331.0, 1021.2, 892.9, 729.7 cm^{-1}. ^{1}H-NMR (500 MHz, DMSO-d_6): δ 8.10 (2H, m, H5, H8), 7.73 (2H, m, H6, H7), 6.16 (1H, s, H3), 4.06 (2H, t, J = 6.0 Hz, H1′), 3.64 (2H, t, J = 6.23 Hz, H4′), 2.05 (4H, m, H2′, H3′). ^{13}C-NMR (125 MHz, DMSO-d_6): δ 184.97, 180.01, 159.65, 134.29, 133.35, 131.99, 131.14, 126.69, 126.17, 110.32, 68.66, 44.42, 29.03, 25.79. ESI-MS: calcd. for $C_{14}H_{13}ClO_3$ [M + H]$^+$: 265.0626, found: 265.0636.

*4.1.2.3. 2-(6-Chlorohexyloxy)naphthalene-1,4-dione (**4c**).* Compound **4c** was obtained from lawsone (**3**) and 1,6-dichlorohexane as described in the general procedure. Yellow solid; yield 85%; IR (KBr): 2941.5, 2856.2, 1683.1, 1645.7, 1247.0, 1014.7, 877.5, 724.3 cm^{-1}. ^{1}H-NMR (500 MHz, DMSO-d_6): δ 8.10 (2H, ddd, J = 0.87, 7.30, 21.04 Hz, H5, H8), 7.73 (2H, m, H6, H7), 6.15 (1H, s, H3), 4.02 (2H, t, J = 6.48 Hz, H1′), 3.56 (2H, t, J = 6.62 Hz, H6′), 1.95−1.79 (4H, m, H2′, H5′), 1.56−1.51 (4H, m, H3′, H4′). ^{13}C-NMR (125 MHz, DMSO-d_6): δ 185.05, 180.14, 159.83, 134.25, 133.30, 132.02, 131.17, 126.69, 126.14, 110.23, 69.37, 44.90, 32.38, 28.16, 26.50, 25.27. ESI-MS: calcd. for $C_{16}H_{17}ClO_3$ [M-H]$^-$: 292.0788, found: 291.0790.

*4.1.2.4. 2-(8-Chlorooctyloxy)naphthalene-1,4-dione (**4d**).* Compound **4d** was obtained from lawsone (**3**) and 1,8-dichlorooctane as described in the general procedure. Yellow solid; yield 80%; IR (KBr): 2919.0, 2854.2, 1683.5, 1643.8, 1248.8, 1022.0, 873.5, 722.6 cm^{-1}. ^{1}H-NMR (500 MHz, DMSO-d_6): δ 8.10 (2H, ddd, J = 0.96, 7.38, 21.57 Hz, H5, H8), 7.73 (2H, m, H6, H7), 6.15 (1H, s, H3), 4.01 (2H, t, J = 6.60 Hz, H1′), 3.54 (2H, t, J = 6.72 Hz, H8′), 1.94−1.86 (2H, m, H2′), 1.82−1.74 (2H, m, H7′), 1.54−1.31 (8H, m, H3′, H4′, H5′, H6′). ^{13}C-NMR (125 MHz, DMSO-d_6): δ 185.08, 180.17, 159.88, 134.24, 133.28, 132.03, 131.19, 126.69, 126.12, 110.21, 69.58, 45.10, 32.57, 29.07, 28.73, 28.23, 26.77, 25.79. ESI-MS: calcd. for $C_{18}H_{21}ClO_3$ [M-H]$^-$: 319.1101, found: 319.1110.

*4.1.3. General Procedure for the Synthesis of Azidoalkyl Derivatives of Lawsone (**5a-5d**).* To a solution of the corresponding chloroalkyl derivatives of lawsone (**4a-4d**, 3.21 mmol) and NaN_3 (9.64 mmol) dissolved in 20 mL of *N*,*N*-dimethylsulfoxide (DMF). The reaction mixture was heated at 120 °C for 2 h. The resulting suspension was then tempered to room temperature with ice-cold water and extracted with diethyl ether (50 mL, three times). The collected organic layer was washed with distilled water (10 mL, two times) and brine (10 mL). Diethyl ether was evaporated, and the product was purified by column chromatography over silica gel to furnish the pure product using hexane:CH_2Cl_2:EtOAc (80:10:10) as the mobile phase and recrystallized from EtOAc. The products were characterized by the corresponding spectroscopic data (^{1}H-NMR, ^{13}C-NMR, and ESI-MS of each compound are in the Supporting Information).

*4.1.3.1. 2-(3-Azidopropoxy)naphthalene-1,4-dione (**5a**).* Compound **5a** was obtained from compound **4a** and NaN_3 as described in the general procedure. Yellow solid; yield 63%; IR (KBr): 3448.2, 2970.1, 2098.8, 1740.1, 1609.2, 1454.3, 1366.4, 1214.7, 1050.6, 722.6 cm^{-1}. ^{1}H-NMR (500 MHz, DMSO-d_6): δ 8.02−7.96 (2H, m, H5, H8), 7.88−7.81 (2H, m, H6, H7), 6.38 (1H, s, H3), 4.13 (2H, t, J = 6.18 Hz, H1′), 3.51 (2H, t, J = 6.71 Hz, H2′), 2.03 (2H, p, J = 6.44 Hz, H3′). ^{13}C-NMR (125 MHz, DMSO-d_6): δ 184.59, 179.55, 159.47, 134.57, 133.70, 131.56, 130.90, 126.15, 125.61, 110.42, 66.42, 47.46, 27.40. ESI-MS: calcd. for $C_{13}H_{11}N_3O_3$ [M + Na]$^+$: 280.0693, found: 280.0694.

*4.1.3.2. 2-(4-Azidobutoxy)naphthalene-1,4-dione (**5b**).* Compound **5b** was obtained from compound **4b** and NaN_3 as described in the general procedure. Yellow solid; yield 70%; IR (KBr): 3448.0, 2942.0, 2097.4, 1740.1, 1607.7, 1456.8, 1364.3, 1210.2, 1042.5, 724.5 cm^{-1}. ^{1}H-NMR (500 MHz, DMSO-d_6): δ 8.03−7.95 (2H, m, H5, H8), 7.88−7.81 (2H, m, H6, H7), 6.38 (1H, s, H3), 4.13 (2H, t, J = 6.18 Hz, H1′), 3.51 (2H, t, J = 6.71 Hz, H2′), 2.50 (2H, m, H3′), 2.03 (2H, quin, J = 6.44 Hz, H4′). ^{13}C-NMR (125 MHz, DMSO-d_6): δ 184.60, 179.56, 159.47, 134.58, 133.72, 131.57, 130.90, 126.16, 125.62, 110.42, 66.43, 47.47, 27.41. ESI-MS: calcd. for $C_{14}H_{13}N_3O_3$ [M + Na]$^+$: 294.0849, found: 294.0850.

*4.1.3.3. 2-(6-Azidohexyloxy)naphthalene-1,4-dione (**5c**).* Compound **5c** was obtained from compound **4c** and NaN_3 as described in the general procedure. Yellow solid; yield 61%; IR (KBr): 3446.8, 2938.9, 2096.0, 1651.8, 1607.2, 1459.2, 1326.5, 1242.9, 1016.9, 725.4 cm^{-1}. ^{1}H-NMR (500 MHz, DMSO-d_6): δ 8.03−7.94 (2H, m, H5, H8), 7.88−7.81 (2H, m, H6, H7), 6.35 (1H, s, H3), 4.05 (2H, t, J = 6.47 Hz, H1′), 2.50 (2H, m, H2′), 1.81−1.74 (2H, m, H3′), 1.59−1.53 (2H, m, H4′), 1.47−1.35 (4H, m, H5′, H6′). ^{13}C-NMR (125 MHz, DMSO-d_6): δ 184.54, 179.63, 159.66, 134.48, 133.59, 131.54, 130.87, 126.08, 125.52, 110.19, 69.16, 50.56, 28.13, 27.69, 25.74, 24.89. ESI-MS: calcd. for $C_{16}H_{17}N_3O_3$ [M + Na]$^+$: 322.1162, found: 322.1156.

*4.1.3.4. 2-(8-Azidooctyloxy)naphthalene-1,4-dione (**5d**).* Compound **5d** was obtained from compound **4d** and NaN_3 as described in the general procedure. Yellow solid; yield 59%; IR (KBr): 3422.4, 2933.8, 2094.8, 1651.3, 1606.4, 1464.5, 1330.1, 1242.8, 1016.5, 724.7 cm^{-1}. ^{1}H-NMR (500 MHz, DMSO-d_6): δ 7.99 (2H, ddd, J = 1.27, 7.35, 18.30 Hz, H5, H8), 7.88−7.81 (2H, m, H6, H7), 6.34 (1H, s, H3), 4.04 (2H, t, J = 6.60 Hz, H1′), 3.31 (2H, t, J = 6.72 Hz, H2′), 1.79−1.73 (2H, m, H7′), 1.56−1.50 (2H, m, H8′), 1.45−1.30 (2H, m, H3′, H4′, H5′, H6′). ^{13}C-NMR (125 MHz, DMSO-d_6): δ 184.54, 179.64, 159.88, 134.48, 133.59, 131.55, 130.87, 126.08, 125.52, 110.19, 69.26, 50.61, 28.48, 28.43, 28.21, 27.80, 26.07, 25.26. ESI-MS: calcd. for $C_{18}H_{21}N_3O_3$ [M + Na]$^+$: 350.1475, found: 350.1471.

https://doi.org/10.1021/acsomega.3c02683
ACS Omega 2023, 8, 32498−32511

*4.1.4. General Procedure for the Synthesis of Lawsone–Quinoxaline Hybrids (**6a-8d**).* A mixture of the corresponding azidoalkyl derivatives of lawsone (**5a-5d**, 3.32 mmol) and the corresponding *N*-(prop-2-ynyl)naphthalen-2-amine derivatives (**2a-2c**, 3.32 mmol) was dissolved in ethanol (EtOH, 25 mL) in a round bottom flask under a nitrogen atmosphere. Then, copper powder (10 mg) and $CuSO_4{\cdot}5H_2O$ (2 mL) were added to the mixture, and it was continued for 24−48 h. After the reaction was monitored by thin layer chromatography, the reaction was terminated. The solid was removed by filtration, the solvent was evaporated under vacuum, and the product was purified by silica gel column chromatography using CH_2Cl_2:MeOH (98:2) as the mobile phase and recrystallization by dichloromethane and hexane. The products were characterized by the corresponding spectroscopic data (^{1}H-NMR, ^{13}C-NMR, and ESI-MS data of each compound are available in the Supporting Information).

*4.1.4.1. 2-(3-(5-((Quinoxalin-6-ylamino)methyl)-1H-1,2,3-triazol-1-yl)propoxy)naphthalene-1,4-dione (**6a**).* Compound **6a** was obtained from compound **2a** and compound **5a** as described in the general procedure. Red solid; yield 38%; IR (KBr): 3438.4, 3291.5, 3138.9, 2943.5, 1686.5, 1649.1, 1603.2, 1439.7, 1333.0, 1207.4, 1023.6, 785.1 cm^{-1}. ^{1}H-NMR (500 MHz, DMSO-d_6): δ 8.59 (1H, d, J = 1.98 Hz, H3″), 8.44 (1H, d, J = 1.98 Hz, H2″), 8.12 (1H, s, H5″), 8.00−7.96 (2H, m, H5, H8), 7.87−7.83 (2H, m, H6, H7), 7.72 (1H, d, J = 9.12 Hz, triazole), 7.33 (1H, dd, J = 2.58, 9.14 Hz, H8″), 7.08 (1H, t, J = 5.60 Hz, NH), 6.86 (1H, d, J = 2.54 Hz, H6″), 6.30 (1H, s, H3), 4.51 (2H, t, J = 6.91 Hz, CH_2-NH), 4.44 (2H, d, J = 5.59 Hz, H1′), 4.04 (2H, t, J = 6.14 Hz, H3′), 2.32 (2H, p, J = 6.52 Hz, H2′). ^{13}C-NMR (125 MHz, DMSO-d_6): δ 184.56, 179.52, 159.40, 149.51, 145.00, 144.77, 139.97, 136.94, 134.59, 133.73, 131.56, 130.89, 129.42, 126.16, 125.63, 123.34, 122.61, 110.39, 102.18, 66.20, 46.27, 38.41, 28.78. ESI-MS: calcd. for $C_{24}H_{20}N_6O_3$ [M + Na]$^+$: 463.1489, found: 463.1489.

*4.1.4.2. 2-(4-(5-((Quinoxalin-6-ylamino)methyl)-1H-1,2,3-triazol-1-yl)butoxy)naphthalene-1,4-dione (**6b**).* Compound **6b** was obtained from compound **2a** and compound **5b** as described in the general procedure. Yellow solid; yield 46%; IR (KBr): 3428.5, 3340.8, 3126.0, 2929.7, 1679.5, 1611.3, 1529.2, 1440.5, 1306.4, 1210.2, 1009.4, 854.4 cm^{-1}. ^{1}H-NMR (500 MHz, DMSO-d_6): δ 8.60 (1H, d, J = 1.97 Hz, H3″), 8.45 (1H, d, J = 1.97 Hz, H2″), 8.10 (1H, s, H5″), 7.98 (2H, ddd, J = 1.23, 7.34, 13.01 Hz, H5, H8), 7.87−7.81 (2H, m, H6, H7), 7.73 (1H, d, J = 9.11 Hz, triazole), 7.34 (1H, dd, J = 2.57, 9.14 Hz, H8″), 7.10 (1H, t, J = 5.62 Hz, NH), 6.87 (1H, d, J = 2.53 Hz, H6″), 6.31 (1H, s, H3), 4.45−4.42 (4H, m, H1′, CH_2-NH), 4.04 (2H, t, J = 6.33 Hz, H4′), 1.98−1.92 (2H, m, H3′), 1.74−1.69 (2H, m, H2′). ^{13}C-NMR (125 MHz, DMSO-d_6): δ 184.62, 179.67, 159.60, 149.55, 145.08, 145.01, 144.60, 139.98, 136.96, 134.59, 133.70, 131.58, 130.90, 129.43, 126.17, 125.62, 123.20, 122.65, 110.28, 102.23, 68.76, 48.90, 38.41, 26.63, 24.81. ESI-MS: calcd. for $C_{25}H_{22}N_6O_3$ [M + Na]$^+$: 477.1646, found: 477.1645.

*4.1.4.3. 2-(6-(5-((Quinoxalin-6-ylamino)methyl)-1H-1,2,3-triazol-1-yl)hexyloxy)naphthalene-1,4-dione (**6c**).* Compound **6c** was obtained from compound **2a** and compound **5c** as described in the general procedure. Yellow solid; yield 73%; IR (KBr): 3490.8, 3390.7, 3125.8, 2945.0, 1680.3, 1605.6, 1519.9, 1463.7, 1345.9, 1243.4, 1021.4, 722.1 cm^{-1}. ^{1}H-NMR (500 MHz, DMSO-d_6): δ 8.62 (1H, d, J = 1.98 Hz, H3″), 8.46 (1H, d, J = 1.98 Hz, H2″), 8.06 (1H, s, H5″), 8.00−7.95 (2H, m, H5, H8), 7.85−7.72 (2H, m, H6, H7), 7.73 (1H, d, J = 9.11 Hz, triazole), 7.31 (1H, dd, J = 2.58, 9.14 Hz, H8″), 7.09 (1H, t, J = 5.62 Hz, NH), 6.86 (1H, d, J = 2.55 Hz, H6″), 6.32 (1H, s, H3), 4.44 (2H, d, J = 5.60 Hz, CH_2-NH), 4.33 (2H, t, J = 7.02 Hz, H1′), 3.99 (2H, t, J = 6.47 Hz, H6′), 1.84−1.67 (4H, m, H2′, H5′), 1.42−1.23 (4H, m, H3′, H4′). ^{13}C-NMR (125 MHz, DMSO-d_6): δ 184.55, 179.64, 159.65, 149.48, 145.05, 144.96, 144.49, 139.91, 136.91, 134.49, 133.60, 131.55, 130.87, 129.36, 126.10, 125.54, 122.94, 122.60, 110.17, 102.17, 69.11, 49.21, 38.38, 29.61, 27.60, 25.41, 24.72. ESI-MS: calcd. for $C_{27}H_{26}N_6O_3$ [M + Na]$^+$: 505.1959, found: 505.1957.

*4.1.4.4. 2-(8-(5-((Quinoxalin-6-ylamino)methyl)-1H-1,2,3-triazol-1-yl)octyloxy)naphthalene-1,4-dione (**6d**).* Compound **6d** was obtained from compound **2a** and compound **5d** as described in the general procedure. Brown solid; yield 92%; IR (KBr): 3398.2, 2929.5, 1677.9, 1606.7, 1524.4, 1436.4, 1353.6, 1210.1, 1017.9, 724.9 cm^{-1}. ^{1}H-NMR (500 MHz, DMSO-d_6): δ 8.62 (1H, d, J = 1.98 Hz, H3″), 8.46 (1H, d, J = 1.98 Hz, H2″), 8.01 (1H, s, H5″), 8.01−7.96 (2H, m, H5, H8), 7.87−7.80 (2H, m, H6, H7), 7.73 (1H, d, J = 9.11 Hz, triazole), 7.34 (1H, dd, J = 2.58, 9.14 Hz, H8″), 7.09 (1H, t, J = 5.63 Hz, NH), 6.86 (1H, d, J = 2.54 Hz, H6″), 6.33 (1H, s, H3), 4.44 (2H, d, J = 5.62 Hz, CH_2-NH), 4.32 (2H, t, J = 7.01 Hz, H1′), 4.01 (2H, t, J = 6.51 Hz, H8′), 1.81−1.69 (4H, m, H2′, H7′), 1.37−1.17 (8H, m, H3′, H4′, H5′, H6′). ^{13}C-NMR (125 MHz, DMSO-d_6): δ 184.55, 179.65, 159.67, 149.46, 145.04, 144.93, 144.48, 139.90, 136.90, 134.48, 133.59, 131.55, 130.87, 129.35, 126.09, 125.52, 122.89, 122.59, 110.18, 102.18, 69.24, 49.25, 38.35, 29.70, 28.40, 28.25, 27.77, 25.73, 25.22. ESI-MS: calcd. for $C_{29}H_{30}N_6O_3$ [M + Na]$^+$: 533.2272, found: 533.2272.

*4.1.4.5. 2-(3-(5-((3-Phenylquinoxalin-6-ylamino)methyl)-1H-1,2,3-triazol-1-yl)propoxy) naphthalene-1,4-dione (**7a**).* Compound **7a** was obtained from compound **2b** and compound **5a** as described in the general procedure. Orange solid; yield 58%; IR (KBr): 3446.2, 2929.0, 1737.6, 1620.9, 1498.5, 1436.0, 1366.2, 1227.8, 1021.8, 780.8 cm^{-1}. ^{1}H-NMR (500 MHz, DMSO-d_6): δ 9.24 (1H, s, H3″), 8.20−8.17 (2H, m, H5, H8), 8.15 (1H, s, H5″), 8.00 (1H, dd, J = 1.50, 7.41 Hz, H6), 7.95 (1H, dd, J = 1.46, 7.44 Hz, H7), 7.87−7.80 (2H, m, H1‴, H5‴), 7.78 (1H, d, J = 9.10 Hz, triazole), 7.54 (2H, d, J = 4.69, 10.31 Hz, H2‴, H4‴), 7.49−7.45 (1H, m, H3‴), 7.36 (1H, dd, J = 2.55, 9.14 Hz, H8″), 7.14 (1H, t, J = 5.60 Hz, NH), 6.91 (1H, d, J = 5.60 Hz, H6″), 6.30 (1H, s, H3), 4.52 (2H, t, J = 6.90 Hz, CH_2-NH), 4.47 (2H, d, J = 5.53 Hz, H1′), 4.05 (2H, t, J = 6.15 Hz, H3′), 2.33 (2H, p, J = 6.61 Hz, H2′). ^{13}C-NMR (125 MHz, DMSO-d_6): δ 184.48, 179.44, 159.34, 149.45, 145.74, 144.72, 143.80, 142.75, 136.81, 135.85, 134.51, 133.65, 131.50, 130.84, 129.57, 129.13, 128.96, 126.43, 126.09, 125.57, 123.33, 110.36, 102.12, 66.15, 46.22, 38.41, 28.74. ESI-MS: calcd. for $C_{30}H_{24}N_6O_3$ [M + Na]$^+$: 539.1802, found: 539.1805.

*4.1.4.6. 2-(4-(5-((3-Phenylquinoxalin-6-ylamino)methyl)-1H-1,2,3-triazol-1-yl)butoxy) naphthalene-1,4-dione (**7b**).* Compound **7b** was obtained from compound **2b** and compound **5b** as described in the general procedure. Yellow solid; yield 50%; IR (KBr): 3431.6, 2928.0, 1715.4, 1621.9, 1498.0, 1454.3, 1366.9, 1226.0, 1053.7, 756.3 cm^{-1}. ^{1}H-NMR (500 MHz, DMSO-d_6): δ 9.25 (1H, s, H3″), 8.19−8.17 (2H, m, H5, H8), 8.12 (1H, s, H5″), 7.96 (2H, ddd, J = 1.25, 7.42, 12.46 Hz, H6, H7), 7.86−7.78 (3H, m, H1‴, H5‴, triazole), 7.53 (2H, dd, J = 4.68, 10.27 Hz, H2‴, H4‴), 7.48−7.46 (1H, m, H3‴), 7.37 (1H, dd, J = 2.55, 9.14 Hz, H8″), 7.16 (1H, t, J

https://doi.org/10.1021/acsomega.3c02683
ACS Omega 2023, 8, 32498−32511

= 5.62 Hz, NH), 6.92 (1H, d, J = 2.50 Hz, H6″), 6.31 (1H, s, H3), 4.48 (2H, d, J = 5.56 Hz, CH_2-NH), 4.44 (2H, t, J = 7.00 Hz, H1′), 4.04 (2H, t, J = 6.30 Hz, H3′), 1.99−1.93 (2H, m, H3′), 1.75−1.69 (2H, m, H2′). ^{13}C-NMR (125 MHz, DMSO-d_6): δ 184.51, 179.47, 159.35, 149.46, 145.78, 144.75, 143.80, 142.77, 136.82, 135.87, 134.54, 133.68, 131.51, 130.85, 129.59, 129.16, 128.99, 126.45, 126.12, 125.59, 123.35, 110.37, 102.14, 66.16, 46.24, 38.43, 28.75. ESI-MS: calcd. for $C_{31}H_{26}N_6O_3$ [M + Na]$^+$: 553.1959, found: 553.1960.

*4.1.4.7. 2-(6-(5-((3-Phenylquinoxalin-6-ylamino)methyl)-1H-1,2,3-triazol-1-yl)hexyloxy) naphthalene-1,4-dione (**7c**).* Compound **7c** was obtained from compound **2b** and compound **5c** as described in the general procedure. Yellow solid; yield 77%; IR (KBr): 3421.3, 2929.4, 1681.0, 1606.7, 1437.9, 1359.8, 1331.4, 1240.8, 1053.8, 781.8 cm^{-1}. ^{1}H-NMR (500 MHz, DMSO-d_6): δ 9.26 (1H, s, H3″), 8.21−8.15 (2H, m, H5, H8), 8.07 (1H, s, H5″), 7.97 (2H, ddd, J = 1.24, 7.35, 16.14 Hz, H6, H7), 7.88−7.77 (3H, m, triazole, H2‴, H4‴), 7.50 (2H, t, J = 7.51 Hz, H1‴, H5‴), 7.44 (1H, m, H3‴), 7.37 (1H, dd, J = 2.55, 9.14 Hz, H8″), 7.15 (1H, t, J = 5.62 Hz, NH), 6.90 (1H, d, J = 2.51 Hz, H6″), 6.29 (1H, s, H3), 4.47 (2H, d, J = 5.57 Hz, CH_2-NH), 4.34 (2H, t, J = 6.97 Hz, H1′), 3.96 (2H, t, J = 7.97 Hz, H6′), 1.87−1.61 (4H, m, H2′, H5′), 1.42−1.21 (4H, m, H3′, H4′). ^{13}C-NMR (125 MHz, DMSO-d_6): δ 184.55, 179.63, 159.63, 149.48, 145.76, 144.54, 143.82, 142.77, 136.79, 135.88, 134.50, 133.61, 131.56, 130.87, 129.58, 129.14, 128.97, 126.42, 126.11, 125.55, 123.00, 110.16, 102.20, 69.12, 49.26, 38.44, 29.63, 27.63, 25.44, 24.74. ESI-MS: calcd. for $C_{33}H_{30}N_6O_3$ [M + Na]$^+$: 581.2272, found: 581.2266.

*4.1.4.8. 2-(8-(5-((3-Phenylquinoxalin-6-ylamino)methyl)-1H-1,2,3-triazol-1-yl)octyloxy) naphthalene-1,4-dione (**7d**).* Compound **7d** was obtained from compound **2b** and compound **5d** as described in the general procedure. Yellow solid; yield 49%; IR (KBr): 3431.9, 2926.0, 1713.2, 1621.2, 1523.2, 1437.2, 1363.9, 1239.5, 1048.8, 778.4 cm^{-1}. ^{1}H-NMR (500 MHz, DMSO-d_6): δ 9.26 (1H, s, H3″), 8.19 (2H, d, H5, H8), 8.06 (1H, s, H5″), 7.97 (2H, ddd, J = 1.00, 7.30, 16.97 Hz, H6, H7), 7.87−7.80 (3H, m, triazole, H2‴, H4‴), 7.52 (2H, t, J = 7.62 Hz, H1‴, H5‴), 7.44 (1H, t, J = 7.32 Hz, H3‴), 7.37 (1H, dd, J = 2.51, 9.13 Hz, H8″), 7.15 (1H, t, J = 5.60 Hz, NH), 6.91 (1H, d, J = 2.40 Hz, H6″), 6.30 (1H, s, H3), 4.47 (2H, d, J = 5.55 Hz, CH_2-NH), 4.34 (2H, t, J = 6.98 Hz, H1′), 3.97 (2H, t, J = 6.52 Hz, H8′), 1.81−1.66 (4H, m, H2′, H7′), 1.28−1.15 (8H, m, H3′, H4′, H5′, H6′). ^{13}C-NMR (125 MHz, DMSO-d_6): δ 184.54, 179.63, 159.65, 149.45, 145.72, 144.50, 143.81, 142.74, 136.78, 135.85, 134.48, 133.59, 131.54, 130.86, 129.55, 129.12, 128.96, 127.11, 126.40, 126.40, 122.94, 110.16, 102.19, 69.23, 49.27, 38.40, 29.70, 28.41, 28.25, 27.77, 25.72, 25.21. ESI-MS: calcd. for $C_{35}H_{34}N_6O_3$ [M + Na]$^+$: 609.2585, found: 609.2583.

*4.1.4.9. 2-(3-(5-((2,3-Dimethylquinoxalin-6-ylamino)-methyl)-1H-1,2,3-triazol-1-yl)propoxy) naphthalene-1,4-dione (**8a**).* Compound **8a** was obtained from compound **2c** and compound **5a** as described in the general procedure. Orange solid; yield 68%; IR (KBr): 3393.9, 2928.2, 1680.9, 1680.6, 1516.1, 1437.8, 1339.5, 1242.7, 1045.4, 781.9 cm^{-1}. ^{1}H-NMR (500 MHz, DMSO-d_6): δ 8.10 (1H, s, H5″), 8.01−7.95 (2H, m, H5, H8), 7.88−7.81 (2H, m, H6, H7), 7.59 (1H, d, J = 9.02 Hz, triazole), 7.17 (1H, dd, J = 2.55, 9.01 Hz, H8″), 6.79 (2H, d, J = 4.08, 7.36 Hz, NH, H6″), 6.27 (1H, s, H3), 4.50 (2H, t, J = 6.90 Hz, CH_2-NH), 4.40 (2H, d, J = 5.60 Hz, H1′), 4.03 (2H, t, J = 6.15 Hz, H3′), 2.52 (6H, s, 2 × CH_3), 2.31 (2H, p, J = 6.51 Hz, H2′). ^{13}C-NMR (125 MHz, DMSO-d_6): δ 184.50, 179.48, 159.36, 152.81, 147.71, 145.09, 142.85, 134.60, 134.57, 133.71, 131.53, 130.86, 128.27, 126.14, 125.61, 123.27, 120.67, 110.35, 102.35, 68.17, 46.22, 38.55, 28.76, 22.60, 22.10. ESI-MS: calcd. for $C_{26}H_{24}N_6O_3$ [M + Na]$^+$: 491.1802, found: 491.1801.

*4.1.4.10. 2-(4-(5-((2,3-Dimethylquinoxalin-6-ylamino)-methyl)-1H-1,2,3-triazol-1-yl)butoxy) naphthalene-1,4-dione (**8b**).* Compound **8b** was obtained from compound **2c** and compound **5b** as described in the general procedure. Yellow solid; yield 45%; IR (KBr): 3395.5, 2921.1, 1681.5, 1607.8, 1516.0, 1442.0, 1340.8, 1242.5, 1046.3, 780.7 cm^{-1}. ^{1}H-NMR (500 MHz, DMSO-d_6): δ 8.08 (1H, s, H5′), 7.99−7.95 (2H, m, H5, H8), 7.87−7.80 (2H, m, H6, H7), 7.59 (1H, d, J = 9.01 Hz, triazole), 7.18 (1H, dd, J = 2.55, 9.01 Hz, H8″), 6.82−6.78 (2H, m, NH, H6″), 6.29 (1H, s, H3), 4.42 (4H, dd, J = 6.25, 13.05 Hz, H1′, CH_2-NH), 4.03 (2H, t, J = 6.33 Hz, H4′), 2.53 (6H, s, 2 × CH_3), 1.98−1.92 (2H, m, H3′), 1.73−1.67 (2H, m, H2′). ^{13}C-NMR (125 MHz, DMSO-d_6): δ 184.57, 179.59, 159.55, 152.80, 148.61, 147.69, 144.90, 142.85, 134.59, 134.56, 133.66, 131.55, 130.85, 128.26, 126.13, 125.58, 123.16, 120.69, 110.22, 102.42, 68.76, 48.85, 38.55, 26.64, 24.75, 22.61, 22.09. ESI-MS: calcd. for $C_{27}H_{26}N_6O_3$ [M + Na]$^+$: 505.1959, found: 505.1959.

*4.1.4.11. 2-(6-(5-((2,3-Dimethylquinoxalin-6-ylamino)-methyl)-1H-1,2,3-triazol-1-yl)hexyloxy)-naphthalene-1,4-dione (**8c**).* Compound **8c** was obtained from compound **2c** and compound **5c** as described in the general procedure. Yellow solid; yield 61%; IR (KBr): 3407.2, 2921.1, 1717.2, 1650.9, 1607.5, 1365.8, 1242.8, 1206.1, 1018.4, 882.1 cm^{-1}. ^{1}H-NMR (500 MHz, DMSO-d_6): δ 8.04 (1H, s, H5′), 7.99−7.95 (2H, m, H5, H8), 7.87−7.80 (2H, m, H6, H7), 7.60 (1H, d, J = 9.02 Hz, triazole), 7.18 (1H, dd, J = 2.56, 9.04 Hz, H8″), 6.81−6.78 (2H, m, NH, H6″), 6.31 (1H, s, H3), 4.39 (2H, d, J = 5.61 Hz, CH_2-NH), 4.33 (2H, t, J = 7.01 Hz, H1′), 3.98 (2H, t, J = 6.47 Hz, H6′), 2.53 (6H, d, J = 11.87 Hz, 2 × CH_3), 1.84−1.66 (4H, m, H2′, H5′), 1.42−1.23 (4H, m, H3′, H4′). ^{13}C-NMR (125 MHz, DMSO-d_6): δ 184.52, 179.60, 159.62, 152.73, 148.58, 147.62, 144.82, 142.84, 134.57, 134.48, 133.59, 131.53, 130.85, 128.21, 126.08, 125.53, 122.86, 120.66, 110.15, 102.34, 69.09, 49.18, 38.52, 29.59, 27.58, 25.39, 24.70, 22.57, 22.07. ESI-MS: calcd. for $C_{29}H_{30}N_6O_3$ [M + Na]$^+$: 533.2272, found: 533.2272.

*4.1.4.12. 2-(8-(5-((2,3-Dimethylquinoxalin-6-ylamino)-methyl)-1H-1,2,3-triazol-1-yl)octyloxy)-naphthalene-1,4-dione (**8d**).* Compound **8d** was obtained from compound **2c** and compound **5d** as described in the general procedure. Yellow solid; yield 50%; IR (KBr): 3438.4, 2929.0, 1714.9, 1607.7, 1515.5, 1341.3, 1242.6, 1154.5, 1019.3, 827.6 cm^{-1}. ^{1}H-NMR (500 MHz, DMSO-d_6): δ 8.03−7.84 (5H, m, H5, H8, H5′, H6, H7), 7.60 (1H, d, J = 9.0 Hz, triazole), 7.18 (1H, dd, J = 2.55, 9.04 Hz, H8″), 6.79 (2H, m, NH, H6″), 6.32 (1H, s, H3), 4.39 (2H, d, J = 5.63 Hz, CH_2-NH), 4.31 (2H, t, J = 7.0 Hz, H1′), 4.00 (2H, t, J = 6.52 Hz, H8′), 2.53 (6H, d, J = 9.41 Hz, 2 × CH_3), 1.74 (4H, m, H2′, H7′), 1.26 (8H, m, H3′, H4′, H5′, H6′). ^{13}C-NMR (125 MHz, DMSO-d_6): δ 184.59, 179.69, 159.70, 152.78, 148.61, 144.85, 142.86, 134.60, 134.53, 133.64, 130.89, 128.24, 126.13, 125.57, 122.88, 120.70, 110.21, 102.40, 69.28, 49.29, 38.54, 29.72, 28.42, 28.27, 27.79, 25.76, 25.24, 22.61, 22.10. ESI-MS: calcd. for $C_{31}H_{34}N_6O_3$ [M + Na]$^+$: 561.2585, found: 561.2583.

4.2. Biological Materials and Methods. *4.2.1. In Vitro AChE and BChE Inhibition Assay.* The cholinesterase

https://doi.org/10.1021/acsomega.3c02683
ACS Omega 2023, 8, 32498−32511

inhibition was evaluated by the Ellman assay. Human recombinant AChE and equine serum BChE were used for the cholinesterase inhibition experiments. Acetylthiocholine iodide (ATChI) and butyrylthiocholine iodide (BTChI) were used as the substrates of the assays, respectively. Test compounds were dissolved in absolute EtOH. The assay solution consisted of 25 μL of 1.5 mM ACTI or 25 μL of 1.5 mM BTChI, 50 μL of 50 mM phosphate buffer (pH 8), 125 μL of 3 mM 5,5-dithiobis-(2-nitrobenzic acid) (DTNB), and 25 μL of 100 μM of test compounds. Then, 25 μL of *Hu*AChE and equine serum of BChE in 50 mM Tris-HCl buffer contained 0.1% (w/v) BSA (pH 8). Reactions were initiated by the addition of the enzyme into the medium. The production of the yellow of 5-thio-2-nitrobenzoic was measured with a microplate reader at 405 nm every 11 s for 2 min. Each experiment was repeated in triplicate. In this study, tacrine and donepezil were used as reference drugs. Percent inhibition and enzyme activities were calculated using the following formulas: % inhibition = [(mean velocity of blank − mean velocity of the sample) × 100]/mean velocity of blank. The IC_{50} value is defined as the concentration of the test compounds required to inhibit AChE and BChE by 50%. This experiment was calculated using GraphPad Prism 2.01 software. The selectivity of AChEI activity of the compounds can be calculated by the ratio between IC_{50} of *Eq*BChE and IC_{50} of *Hu*AChE and shown as the selectivity index (SI).[41]

4.2.2. Kinetic Characterization of AChE Inhibitory Activity. The kinetic study for the AChE inhibition by compound **6d** was carried out according to the Ellman assay using four different concentrations of the inhibitor (0, 4, 7.5, and 15 μM). The Lineweaver−Burk plot was generated by plotting 1/[V] against 1/[S] at variable concentrations of substrates (ATChI: 0.5, 1.5, 2.5, 5, and 10 μM). Then, mode of inhibition can be determined from the variation of K_m and V_{max} by the Prism program.[42]

4.2.3. SRB Assay. Human neuroblastoma SH-SY5Y cells were maintained in Dulbecco's modified Eagle's medium (DMEM) supplemented with 10% fetal bovine serum (FBS), located at 37 °C in a humidified atmosphere containing 5% CO_2, changed every 2−3 days. Cell viability was determined using a sulforhodamine B (SRB) assay. SH-SY5Y cells were seeded into a 96-well plate at 10,000 cells/well, incubated at 37 °C in a humid 5% CO_2 atmosphere for 24 h, and treated with or without different concentrations of test compounds (**6a-8d**). After 48 h of incubation, the cells were fixed with 40% (w/v) trichloroacetic acid (TCA). The cells were then incubated at 4 °C for 1 h. SRB solution (100 μL) was added to each well, and the cells were incubated for 1 h at room temperature. The supernatant was discarded, washed three times with 1% glacial acetic acid water, and air-dried. Finally, to each well, 100 μL/well for 10 mM Tris base solution was added, and the OD value was measured at 492 nm using a microplate reader.[43,44]

4.3. *In Silico* Analysis of ChE Binding Characteristics. *4.3.1. Preparation of the Protein Structure.* The AutoDock Tools (ADT) version 1.5.6 program was utilized to conduct docking studies.[45] 7D9O (human recombinant acetylcholinesterase) and 4BDS (human butyrylcholinesterase) were extracted from the RCSB Protein Data Bank (www.rcsb.org)[46] as complexes bound with inhibitors H0L (donepezil analogue)[47] and THA (tacrine). Therefore, water molecules and the original inhibitors were eliminated from both protein structures.

4.3.2. Preparation of Ligands. The lawsone 3D structure file was downloaded from the PubChem database (https://pubchem.ncbi.nlm.nih.gov/). The lawsone structure was taken from a structure with CID 6755, and other ligands were established by the Public Computational Chemistry Database Project (www.pccdb.org) and saved in a mol2 format file, which was then converted into a PDB file using Obabel.[48] Polar hydrogen atoms were added to all ligands. ADT was then used to write the structure into the PDBT format file.

4.3.3. Molecular Docking Study. Molecular docking research was conducted with the AutoDock4 program. In the process, the structure of the protein was fixed as a rigid molecule with a flexible ligand. The active site box of *Hu*AChE and *Hu*BChE has dimensions of 60 × 60 × 60 cubic angstroms ($Å^3$). All maps were generated with a grid point interval of 0.375 Å. The centers of the protein structures of *Hu*AChE (PDB ID: 7D9O) and *Hu*BChE (PDB ID: 4BDS) are located at x = 10.64, y = 48.01, and z = 34.23 and x = 131.88, y = 116.41, and z = 40.78, respectively. AutoDock4 was used to operate a genetic algorithm (GA) with 50 iterations and a population size of 200 using the default parameters. The conformation of the ligand−enzyme with the lowest energy (ΔG values) was measured to analyze the interaction between the inhibitor and enzyme.[49]

4.3.4. Interaction Analysis and Structural Visualization from Molecular Docking. Biovia Discovery Studio package version 2021 and visual molecular dynamics (VMD) package[50] were used for interaction analysis and visualization. For the ligand−protein interactions, the hydrogen bond, $\pi-\pi$ interaction, cation-π interaction, π-alkyl interaction, and cation-π interaction were considered.

4.4. Molecular Dynamics (MD) Simulation. The *Hu*AChE enzyme selected was the PDB structure code 7D9O (a resolution of 2.45 Å).[47] AMBER20 parameters were used for MD simulation to simulate the dynamic aqueous condition. The docked **6d**-*Hu*AChE complex and donepezil-*Hu*AChE in the PDB format were used as starting coordinates. First, the restrained electrostatic atomic partial potential (RESP) charge was parameterized using geometry optimization and electrostatic single-point charge for all ligands, such as compound **6d** and donepezil drug. The process was carried out using the Gaussian16 package's B3LYP/6-31G* calculation.[51]

Second, all protein structures were modeled with AMBER20 parameters, and the protonation state of each ionizable amino acid was determined with the PropKA web server.[52] The protonation of glutamates was set GLH in AMBER name: Glu7, Glu84, Glu202, Glu285, Glu313, Glu450, Glu452, Glu469, Glu491, and Glu519. No protonation of aspartate (Asp) was found. Five doubly protonated histidines (His) were set HIP in AMBER name: His212, His223, His322, His405, and His447. Furthermore, *Hu*AChE includes three disulfide bonds: Cys69-Cys96, Cys257-Cys272, and Cys409-Cys529. The *Hu*AChE, or compound **6d**-*Hu*AChE, and donepezil-*Hu*AChE system were solvated at a 14 Å distance by TIP3P water and neutralized by eight chlorides (Cl^-) using the Leap module. The 40 Na^+Cl^- pairs were added. Finally, the system included a *Hu*AChE, a ligand (compound **6d** and donepezil), 40 Na^+, 48 Cl^-, and 22,294 TIP3P waters, yielding a 0.10 M NaCl solution.

The MD simulation began with the best docked pose from the molecular docking study, like previous studies.[53,54] Under the periodic boundary condition, the steepest descent method for 1000 steps and the conjugate gradient method for 1000

https://doi.org/10.1021/acsomega.3c02683
ACS Omega 2023, 8, 32498−32511

steps were used. To deal with nonbonded/electrostatic interaction, the NVT simulation was set at 298 K (25 °C) with a cutoff of 16 Å. Harmonic restraint was applied to the compound−protein coordinates with force constants of 200, 100, 50, 25, and 10 kcal mol^{-1} $Å^{-2}$. Each force constant lasted for 400 ps with a 1 fs time step, from which a 2 ns simulation was then obtained. The NPT simulation, without positional restraints, was then simulated with a pressure of 1.013 bar. The temperature and pressure were monitored by the weak-coupling algorithm.[55] The simulation lasted for 200 ns, with a time step of 2 fs. The MD simulation was performed using the PMEMD module implemented in AMBER20.

The VMD program achieved the root-mean square displacement (RMSD) calculation of the equidistant 2000 snapshots obtained from the MD trajectory for 200 ns as well as structure visualization. The distance between the ligand and the interested amino acids (Trp80 and Trp280) was calculated using the AMBER20 package's CPPTRAJ module to investigate the $\pi-\pi$ interaction between the sidechain and aromatic ring of the synthesized compound. Using the molecular mechanics/generalized born surface area (MM/GBSA) method, the average binding free energy was calculated.[56] The energy calculation was summarized in the previous study.[57]

■ ASSOCIATED CONTENT

Supporting Information

The Supporting Information is available free of charge at https://pubs.acs.org/doi/10.1021/acsomega.3c02683.

Experimental details, spectroscopic data (^{1}H- and ^{13}C-NMR spectra) of all the new compounds, and molecular docking of compound **6d** and donepezil (PDF)

■ AUTHOR INFORMATION

Corresponding Authors

Varomyalin Tipmanee − *Department of Biomedical Sciences and Biomedical Engineering, Faculty of Medicine, Prince of Songkla University, Hat Yai, Songkhla 90110, Thailand;* orcid.org/0000-0001-6017-7519; Email: tvaromya@medicine.psu.ac.th

Luelak Lomlim − *Department of Pharmaceutical Chemistry, Faculty of Pharmaceutical Sciences and Phytomedicine and Pharmaceutical Biotechnology Excellent Center (PPBEC), Faculty of Pharmaceutical Sciences, Prince of Songkla University, Hat Yai, Songkhla 90110, Thailand;* orcid.org/0000-0003-1229-2189; Email: luelak.l@psu.ac.th

Authors

Paptawan Suwanhom − *Department of Pharmaceutical Chemistry, Faculty of Pharmaceutical Sciences and Phytomedicine and Pharmaceutical Biotechnology Excellent Center (PPBEC), Faculty of Pharmaceutical Sciences, Prince of Songkla University, Hat Yai, Songkhla 90110, Thailand*

Teerapat Nualnoi − *Department of Pharmaceutical Technology, Faculty of Pharmaceutical Sciences, Prince of Songkla University, Hat Yai, Songkhla 90110, Thailand*

Pasarat Khongkow − *Department of Biomedical Sciences and Biomedical Engineering, Faculty of Medicine, Prince of Songkla University, Hat Yai, Songkhla 90110, Thailand*

Complete contact information is available at: https://pubs.acs.org/10.1021/acsomega.3c02683

Notes

The authors declare no competing financial interest.

■ ACKNOWLEDGMENTS

This research was supported by the National Science, Research and Innovation Fund (NSRF) and Prince of Songkla University (grant no. PHA6505110S). We would like to thank Dr. Saffanah Mohd Ab Azid for linguistic proofreading of the manuscript.

■ REFERENCES

(1) "*World Alzheimer Report*, 2021. http://alz.co.uk/research/world-report **2021** (accessed on 27/12/2021).

(2) Tönnies, E.; Trushina, E. Oxidative Stress, Synaptic Dysfunction, and Alzheimer's Disease. *J. Alzheimers Dis.* **2017**, *57*, 1105−1121.

(3) Rajmohan, R.; Reddy, P. H. Amyloid-Beta and Phosphorylated Tau Accumulations Cause Abnormalities at Synapses of Alzheimer's disease Neurons. *J. Alzheimers Dis.* **2017**, *57*, 975−999.

(4) Sussman, J. L.; Harel, M.; Frolow, F.; Oefner, C.; Goldman, A.; Toker, L.; Silman, I. Atomic structure of acetylcholinesterase from *Torpedo californica*: A prototypic acetylcholine-binding protein. *Science* **1991**, *253*, 872−879.

(5) Mesulam, M.; Guillozzet, A.; Shaw, P.; Quinn, N. Widely spread butyrylcholinesterase can hydrolyze acetylcholine in the normal and Alzheimer brain. *Neurobiol. Dis.* **2002**, *9*, 88−93.

(6) Colović, M. B.; Krstić, D. Z.; Lazarević-Pašti, T. D.; Bondžić, A. M.; Vasić, V. . M. Acetylcholinesterase inhibors: pharmacology and toxicology. *Curr. Neuropharmacol.* **2013**, *11*, 315−335.

(7) Arendt, T.; Brückner, M. K.; Lange, M.; Bigl, V. Changes in acetylcholinesterase and butyrylcholinesterase in Alzheimer's disease resemble embryonic development-A study of molecular forms. *Neurochem. Int.* **1992**, *21*, 381−396.

(8) Greig, N. H.; Lahiri, D. K.; Sambamurti, K. Butyrylcholinesterase: An important new target in Alzheimer's disease therapy. *Int. Psychogeriatr.* **2002**, *14*, 77−91.

(9) Holzgrabe, U.; Kapková, P.; Alptüzün, V.; Scheiber, J.; Kugelmann, E. Targeting acetylcholinesterase to treat neurodegeneration. *Expert Opin. Ther. Targets* **2007**, *11*, 161.

(10) Kryger, G.; Silman, I.; Sussman, J. L. Structure of acetylcholinesterase complexed with E2020 (Aricept): implications for the design of new anti-Alzheimer drugs. *Structure* **1999**, *7*, 297.

(11) Muñoz-Torrero, D.; Camps, P. Dimeric and hybrid anti-Alzheimer drug candidates. *Curr. Med. Chem.* **2006**, *13*, 399.

(12) Najafi, Z.; Mahdavi, M.; Saeedi, M.; Kaimpour-Razkenari, E.; Edraki, N.; Sharifzadeh, M.; Khanavi, M.; Akbarzadeh, T. Novel tacrine-coumarin hybrids linked to 1,2,3-triazole as anti-Alzheimer's compounds: In vitro and in vivo biological evaluation and docking study. *Bioorg. Chem.* **2019**, *83*, 303−316.

(13) Gorecki, L.; Uliassi, E.; Bartolini, M.; Janockova, J.; Hrabinova, M.; Hepnarova, V.; Prchal, L.; Muckova, L.; Pejchal, J.; Karasova, J. Z.; Mezeiova, E.; Benkova, M.; Kobrlova, T.; Soukup, O.; Petralla, S.; Monti, B.; Korabecny, J.; Bolognesi, M. L. Phenothiazine-Tacrine Heterodimers: Pursuing Multitarget Directed Approach in Alzheimer's Disease. *ACS Chem. Neurosci.* **2021**, *12*, 1698−1715.

(14) Campora, M.; Canale, C.; Gatta, E.; Tasso, B.; Laurini, E.; Relini, A.; Pricl, S.; Catto, M.; Tonelli, M. Multitarget Biological Profiling of New Naphthoquinone and Anthraquinone-Based Derivatives for the Treatment of Alzheimer's Disease. *ACS Chem. Neurosci.* **2021**, *12*, 447−461.

(15) Wu, G.; Gao, Y.; Kang, D.; Huang, B.; Huo, Z.; Liu, H.; Poongavanam, V.; Zhan, P.; Liu, X. Design, synthesis and biological evaluation of tacrine-1,2,3-triazole derivatives as potent cholinesterase inhibitors. *Med. Chem. Comm.* **2018**, *9*, 149−159.

(16) Fang, J.; Wu, P.; Yang, R.; Gao, L.; Li, C.; Wang, D.; Wu, S.; Liu, A.-L.; Du, G.-H. Inhibition of acetylcholinesterase by two genistein derivatives: Kinetic analysis, molecular docking and molecular dynamics simulation. *Acta Pharm. Sin. B.* **2014**, *4*, 430−437.

(17) Nepovimova, E.; Uliassi, E.; Korabecby, J.; Peña-Altamira, L. E.; Samez, S.; Pesaresi, A.; Garcia, G. E.; Bartolini, M.; Andrisano, V.; Bergamini, C.; Fato, R.; Lamba, D.; Roberti, M.; Kuca, K.; Monti, B.; Bolognesi, M. L. Multitarget Drug Design Strategy: Quinone-Tacrine Hybrids Designed To Block Amyloid-β Aggregation and To Exert Anticholinesterase and Antioxidant Effects. *J. Med. Chem.* **2014**, *57*, 8576−8589.
(18) Singh, A.; Sharma, S.; Arora, S.; Attri, S.; Kaur, P.; Gulati, H. K.; Bhagat, K.; Kumar, N.; Singh, H.; Singh, J. V.; Bedi, P. M. S. New coumarin-benzotriazole based hybrid molecules as inhibitors of acetylcholinesterase and amyloid aggregation. *Bioorg. Med. Chem. Lett.* **2020**, *30*, No. 127477.
(19) Gao, H.; Jiang, Y.; Zhan, J.; Sun, Y. Pharmacophore-based drug design of AChE and BChE dual inhibitors as potential anti-Alzheimer's disease agents. *Bioorg. Chem.* **2021**, *114*, No. 105149.
(20) Zueva, I.; Dias, J.; Lushchekina, S.; Semenov, V.; Mukhamedyarov, M.; Pashirova, T.; Babaev, V.; Nachon, F.; Petrova, N.; Nurullin, L.; Zakharova, L.; Ilyin, V.; Masson, P.; Petrov, K. New evidence for dual binding site inhibitors of acetylcholinesterase as improved drugs for treatment of Alzheimer's disease. *Neuropharmacology* **2019**, *155*, 131−141.
(21) Suwanhom, P.; Seatang, J.; Khongkow, P.; Nualnoi, T.; Tipmanee, V.; Lomlim, L. Synthesis, Biological Evaluation, and *In Silico* Studies of new Acetylcholinesterase Inhibitors Based on Quinoxaline Scaffold. *Molecules* **2021**, *26*, 4895.
(22) Scherzer-Attali, R.; Pellarin, R.; Convertino, M.; Frydman-Marom, A.; Egoz-Matia, N.; Peled, S.; Levy-Sakin, M.; Shalev, D. E.; Caflisch, A.; Gazit, E.; Segal, D. Complete phenotypic recovery of an Alzheimer's disease model by a quinone-tryptophan hybrid aggregation inhibitor. *PLoS One* **2010**, *5*, No. e11101.
(23) Bermejo-Bescós, P.; Martín-Aragón, S.; Jiménez-Aliaga, K. L.; Ortega, A.; Molina, M. T.; Buxaderas, E.; Orellana, G.; Csákÿ, A. G. *In vitro* antiamyloidogenic properties of 1,4-naphthoquinones. *Biochem. Biophys. Res. Commun.* **2010**, *400*, 169−174.
(24) Campora, M.; Francesconi, V.; Schenone, S.; Tasso, B.; Tonelli, M. Journey on Naphthoquinone and Anthraquinone Derivatives: New Insights in Alzheimer's Disease. *Pharmaceuticals* **2021**, *14*, 33.
(25) Riaz, M. T.; Yaqub, M.; Shafiq, Z.; Ashraf, A.; Khalid, M.; Taslimi, P.; Tas, R.; Tuzun, B.; Gulçin, I. Synthesis, biological activity and docking calculations of bis-naphthoquinone derivatives from Lawsone. *Bioorg. Chem.* **2021**, *114*, 105069.
(26) López López, L. I.; Nery Flores, S. D.; Silva Belmares, S. Y.; Sáenz Galindo, A. Naphthoquinones: Biological properties and synthesis of lawsone and derivatives—A structured review. *Vitae* **2015**, *21*, 248−258.
(27) Estolano-Cobián, A.; Noriega-Iribe, E.; Díaz-Rubio, L.; et al. Antioxidant, antiproliferative, and acetylcholinesterase inhibition activity of amino alcohol derivatives from 1,4-naphthoquinone. *Med. Chem. Res.* **2020**, *29*, 1986−1999.
(28) Khelifi, I.; Tourrette, A.; Dhouafli, Z.; Bouajilaj, J.; Efferth, T.; Abdelfatah, S.; Ksouri, R.; Hayouni, E. A. The antioxidant 2,3-dichloro,5,8-dihydroxy,1,4-naphthoquinone inhibits acetyl-cholinesterase activity and amyloid β_{42}aggregation: A dual target therapeutic candidate compound for the treatment of Alzheimer's disease. *Biotechnol. Appl. Biochem.* **2020**, *67*, 983−990.
(29) Nuthakki, V. K.; Choudhary, S.; Reddy, C. N.; Bhatt, S.; Jamwal, A.; Jotshi, A.; Raghuvanshi, R.; Sharma, A.; Thakur, S.; Jadhav, H. R.; Bharate, S. S.; Nandi, U.; Kumar, A.; Bharate, S. B. Design, Synthesis, and Pharmacological Evaluation of Embelin−Aryl/alkyl Amine Hybrids as Orally Bioavailable Blood−Brain Barrier Permeable Multitargeted Agents with Therapeutic Potential in Alzheimer's Disease: Discovery of SB-1448. *ACS Chem. Neurosci.* **2023**, *14*, 1193−1219.
(30) Khan, S. A.; Akhtar, M. .; Gogoi, U.; Meenakshi, D. U.; Das, A. An Overview of 1,2,3-triazole-Containing Hybrids and Their Potential Anticholinesterase Activities. *Pharmaceuticals* **2013**, *16*, 179.
(31) Le Douaron, G.; Schmidt, F.; Amar, M.; Kadar, H.; Debortoli, L.; Latini, A.; Séon-Méniel, B.; Ferrié, L.; Michel, P. P.; Touboul, D.; Brunelle, A.; Raisman-Vozari, R.; Figadère, B. Neuroprotective effects of a brain permeant 6-aminoquinoxaline derivative in cell culture conditions that model the loss of dopaminergic neurons in Parkinson disease. *Eur. J. Med. Chem.* **2015**, *89*, 467−479.
(32) Kara, J.; Suwanhom, P.; Wattanapiromsakul, C.; Nualnoi, T.; Puripattanavong, J.; Khongkow, P.; Lee, V. S.; Gaurav, A.; Lomlim, L. Synthesis of 2-(2-oxo-2H-chromen-4-yl)acetamides as potent acetylcholinesterase inhibitors and molecular insights into binding interactions. *Arch. Pharm.* **2019**, 352.
(33) Kushwaha, K.; Kaushik, N.; Lata; Jain, S. C. Design and synthesis off novel 2*H*-chromene-2one derivatives bearing 1,2,3-triazole moiety as lead antimicrobial. *Bioorg. Med. Chem. Lett.* **2014**, *24*, 1795−1801.
(34) Petrat, w.; Wattanapiromsakul, C.; Nualnol, T.; Sabri, N.H.; Lee, V.S.; Lomlim, L. Cholinesterase Inhibitory Activity, Kinetic and Molecular Docking Studies of N-(1substituted-1*H*-1,2,3-triazole-4-yl)-aralkylamide Derivatives. *Walailak J. Sci. & Technol.* **2017**, *14*, 687−701.
(35) Ellman, G. L.; Courtney, K. D.; Andres, V. J.; Featherstone, R. M. A new and rapid colorimetric determination of acetylcholinesterase activity. *Biochem. Pharmacol.* **1961**, *7*, 88−95.
(36) Suwanhom, P.; Nualnoi, T.; Khongkow, P.; Lee, V. S.; Lomlim, L. Synthesis and evaluation of chromone-2-carboxamido-alkylamines as potent acetylcholinesterase inhibitors. *Med. Chem. Res.* **2020**, *29*, 564−574.
(37) Vicente-Zordo, D.; Rosales-Conrado, N.; León-González, M. E.; Brunetti, L.; Piemontese, L.; Pereira-Santos, A. R.; Cardoso, S. M.; Madrid, Y.; Chaves, A.; Amélia Santos, M. Novel Rivastigmine Derivatives as Promising Multi-Target Compounds for Potential Treatment of Alzheimer's Disease. *Biomedicines* **2022**, *10*, 1510.
(38) Kovalevich, J.; Langford, D. Considerations for the use of SH-SY5Y neuroblastoma cells in neurobiology. *Methods Mol. Biol.* **2013**, *1078*, 9−21.
(39) de Medeiros, L. M.; De Bastiani, M. A.; Rico, E. P.; Schonhofen, P.; Pfaffenseller, B.; Wollenhaupt-Aguiar, B.; Grun, L.; Barbé-Tuana, F.; Zimmer, E. R.; Castro, M. A. A.; Parsons, R. B.; Klamt, F. Cholinergic differentiation of human neuroblastoma SH-SY5Y cell line and its potential use as an in vitro model for Alzheimer's disease studies. *Mol. Neurobiol.* **2019**, *56*, 7355−7367.
(40) Wang, X.; Zhang, M.; Liu, H. LncRNA17A regulates autophagy and apoptosis of SH-SY5Y cell line as an in vitro model for Alzheimer's disease. *Biosci., Biotechnol., Biochem.* **2019**, *83*, 609−621.
(41) Decker, M.; Krauth, F.; Lehmann, J. Novel Tricyclic Quinazolinimines and Related Tetracyclic Nitrogen Bridgehead Compounds as Cholinesterase Inhibitors with Selectivity towards Butyrylcholinesterase. *Bioorg. Med. Chem.* **2006**, *14*, 1966−1977.
(42) Buker, S. M.; Boriack-Sjodin, P. A.; Copeland, R. A. Enzyme-Inhibitor Interactions and a Simple, Rapid Method for Determining Inhibition Modality. *SLAS Discovery* **2019**, *24*, 515−522.
(43) Orellana, E. A.; Kasinski, A. L. Sulforhodamine B (SRB) Assay in Cell Culture to Investigate Cell Proliferation. *Bio-Protoc.* **2016**, *6*(), DOI: 10.21769/BioProtoc.1984.
(44) Skehan, P.; Storeng, R.; Scudiero, D.; Monks, A.; McMahon, J.; Vistica, D.; Warren, J. T.; Bokesch, H.; Kenney, S.; Boyd, M. R. New colorimetric cytotoxicity assay for anticancerdrug screening. *J. Natl. Cancer. Inst.* **1990**, *82*, 1107−1112.
(45) Morris, G. M.; Huey, R.; Lindstrom, W.; Sanner, M. F.; Belew, R. K.; Goodsell, D. S.; Olson, A. J. AutoDock4 and AutoDock-Tools4: Automated docking with selective receptor flexibility. *J. Comput. Chem.* **2009**, *30*, 2785−2791.
(46) Berman, H. M.; Westbrook, J.; Feng, Z.; Gilliland, G.; Bhat, T. N.; Weissig, H.; Shindyalov, I. N.; Bourne, P. E. The Protein Data Bank. *Nucleic Acids Res.* **2000**, *28*, 235−242.
(47) Zhou, Y.; Fu, Y.; Yin, W.; Li, J.; Wang, W.; Bai, F.; Xu, S.; Gong, Q.; Peng, T.; Hong, Y.; Zhang, D.; Zhang, D.; Liu, Q.; Xu, Y.; Xu, H. E.; Zhang, H.; Jiang, H.; Liu, H. Kinetics-Driven Drug Design Strategy for Next-Generation Acetylcholinesterase Inhibitors to Clinical Candidate. *J. Med. Chem.* **2021**, *64*, 1844−1855.

https://doi.org/10.1021/acsomega.3c02683
ACS Omega 2023, 8, 32498−32511

(48) O'Boyle, N. M.; Banck, M.; James, C. A.; Morley, C.; Vandermeersch, T.; Hutchison, G. R. Open Babel: An open chemical toolbox. *Aust. J. Chem.* **2011**, *3*, 33.
(49) Jacob, R. B.; Andersen, T.; McDougal, O. M. Accessible High-Throughput Virtual Screening Molecular Docking Software for Students and Educators. *PLoS Comput. Biol.* **2012**, *8*, No. e100249.
(50) Humphrey, W.; Dalke, A.; Schulten, K. Visual molecular dynamics. *J. Mol. Graphics* **1996**, *14*, 33−38.
(51) Frisch, M. J.; Trucks, G. W.; Schlegel, H. B.; Scuseria, G. E.; Robb, M. A.; Cheeseman, J. R.; Scalmani, G.; Barone, V.; Petersson, G. A.; Nakatsuji, H.; Li, X.; Caricato, M.; Marenich, A. V.; Bloino, J.; Janesko, B. G.; Gomperts, R.; Mennucci, B.; Hratchian, H. P.; Ortiz, J. V.; Izmaylov, A. F.; Sonnenberg, J. L.; Williams-Young, D.; Ding, F.; Lipparini, F.; Egidi, F.; Goings, J.; Peng, B.; Petrone, A.; Henderson, T.; Ranasinghe, D.; Zakrzewski, V. G.; Gao, J.; Rega, N.; Zheng, G.; Liang, W.; Hada, M.; Ehara, M.; Toyota, K.; Fukuda, R.; Hasegawa, J.; Ishida, M.; Nakajima, T.; Honda, Y.; Kitao, O.; Nakai, H.; Vreven, T.; Throssell, K.; Montgomery, J. A., Jr.; Peralta, J. E.; Ogliaro, F.; Bearpark, M. J.; Heyd, J. J.; Brothers, E. N.; Kudin, K. N.; Staroverov, V. N.; Keith, T. A.; Kobayashi, R.; Normand, J.; Raghavachari, K.; Rendell, A. P.; Burant, J. C.; Iyengar, S. S.; Tomasi, J.; Cossi, M.; Millam, J.M.; Klene, M.; Adamo, C.; Cammi, R.; Ochterski, J. W.; Martin, R. L.; Morokuma, K.; Farkas, O.; Foresman, J. B.; Fox, D. J. *Gaussian 16, Revision C.01*, Gaussian, Inc.: Wallingford CT, 2016.
(52) Rostkowski, M.; Olsson, M. H.; Søndergaard, C. R.; Jensen, J. H. Graphical analysis of pH dependent properties of proteins predicted using PROPKA. *BMC Struct. Biol.* **2011**, *11*, 6.
(53) Tanawattanasuntorn, T.; Thongpanchang, T.; Rungrotmongkol, T.; Hanpaibool, C.; Graidist, P.; Tipmanee, V. (−)-Kusunokinin as a Potential Aldose Reductase Inhibitor: Equivalency Observed via AKR1B1 Dynamics Simulation. *ACS Omega* **2021**, *6*, 606−614.
(54) Chompunud Na Ayudhya, C.; Graidist, P.; Tipmanee, V. Potential Stereoselective Binding of Trans-(±)-Kusunokinin and Cis-(±)-Kusunokinin Isomers to CSF1R. *Molecules* **2022**, *27*, 4194.
(55) Berendsen, H. J. C. Transport Properties Computed by Linear Response through Weak Coupling to a Bath. *Comput. Mater. Sci.* **1991**, *205*, DOI: 10.1007/978-94-011-3546-7_7.
(56) Genheden, S.; Ryde, U. The MM/PBSA and MM/GBSA methods to estimate ligand-binding affinities. *Expert Opin. Drug Discovery* **2015**, *10*, 449−461.
(57) Jewboonchu, J.; Saetang, J.; Saeloh, D.; Siriyong, T.; Rungrotmongkol, T.; Voravuthikunchai, S. P.; Tipmanee, V. Atomistic insight and modeled elucidation of conessine towards Pseudomonas aeruginosa efflux pump. *J. Biomol. Struct. Dyn.* **2022**, *40*, 1480−1489.

https://doi.org/10.1021/acsomega.3c02683
ACS Omega 2023, 8, 32498−32511